Self Consistent Random Phase Approximation and the restoration of symmetries within the three-level Lipkin model

D. S. Delion
National Institute of Physics and Nuclear Engineering, Bucharest Măgurele, POB MG-6, Romania

P. Schuck
Institut de Physique Nucléaire, Orsay, 91406 - Orsay CEDEX, France

J. Dukelsky
Instituto de Estructura de la Materia, CSIC, Serrano 123, 28006 Madrid, Spain

(Dated: today)

We show that it is possible to restore the symmetry associated with the Goldstone mode within the Self Consistent Random Phase Approximation (SCRPA) applied to the three-level Lipkin model. We determine one and two-body densities as very convergent expansions in terms of the generators of the RPA basis. We show that SCRPA excitations correspond to the heads of some rotational bands in the exact spectrum. It turns out that the SCRPA eigenmodes for $N = 2$ coincide with exact solutions, given by the diagonalisation procedure.

PACS numbers: 21.60.Jz, 24.10.Cn
Keywords: Selfconsistent Random Phase Approximation, Three level Lipkin model, Goldstone mode

arXiv:nucl-th/0405002v1 3 May 2004

I. INTRODUCTION

The Random Phase Approximation (RPA) is one of the most popular microscopic approaches to describe collective excitations in interacting many body problems [1, 2, 3, 4, 5]. For example it is widely used in condensed matter physics [2, 3, 4], mainly to calculate the excitation spectrum via the linear response function. However, RPA is equally common in nuclear physics and other systems of finite size like cold atoms in traps [5, 6, 7], or metallic clusters [8], etc. In these various fields RPA has slightly different meaning. We here will use it in the most general sense, like it is mostly employed e.g. in nuclear physics, including exchange, as it appears in linearising the time dependent Hartree-Fock equations around equilibrium [1, 5]. Besides its relative simplicity, both conceptually and for numerical applications, RPA also has very desirable properties: when it is evaluated in the Hartree-Fock (HF) basis, then the f-sum rule and conservation laws are fulfilled, even and in fact most importantly in cases with spontaneously broken symmetries. For example in nuclear physics, where HF always breaks translational invariance, the corresponding RPA restores the symmetry in producing a Goldstone mode at zero energy [1, 5]. The same happens when other symmetries, like rotation (deformation) and particle number symmetries (superfluidity) are broken. Unfortunately, when going beyond the HF-RPA scheme, the situation with respect to symmetry restoration and conservation laws is much less clear. Though there exists the well-known concept proposed by Kadanoff and Baym of the Φ-derivable functional [9], which formally maintains all these properties, in practice any approach beyond HF-RPA faces serious difficulties. This stems essentially from the fact that in this scheme going beyond RPA is equivalent to introduce an integral kernel depending on more than one energy variable corresponding to the s,u, and t-channels of relativistic field theory. This then complicates the numerical task enormously.

On the other hand, in certain circumstances one has to go beyond RPA because this approach also has a number of inherent quite severe drawbacks. For example it is well known that RPA violates the Pauli principle (the famous "quasi boson approximation"). This can induce strong errors and even give rise to qualitatively wrong results, as for example in the multilevel pairing Hamiltonian with Kramer's degeneracy, which is very much used recently for the description of superconducting nano grains [10].

A related problem which immediately appears when giving a close look to RPA is its lack of consistency. For example in the bubble summation one calculates the correlation energy of an electron gas [4] but in the RPA-equation occupation numbers $n_k^{(0)} = \{0, 1\}$ are used which correspond to an uncorrelated (HF) ground state. It seems obvious that, at least for the occupation numbers, a correlated ground state should be used. The corresponding approach already will contain RPA correlations self-consistently. This has become increasingly popular in recent years, and it has been called renormalised RPA (r-RPA) [11, 12, 13]. Lately r-RPA was widely and successfully used in describing the double beta decay process [14, 15, 16] and the electronic properties of the metal clusters [8].

In fact r-RPA is an approximation to a more general extension of the RPA which is called Self-Consistent RPA (SCRPA) [17], or also Cluster Hartree-Fock (CHF) [18].

We recently had quite remarkable success with SCRPA in a number of non trivial problems [10, 19, 20].

In this paper we will specifically investigate the properties of SCRPA with respect to conservation laws and restoration of symmetries, the fulfilement of which is, as already mentioned, one of the outstanding aspects of standard RPA theory. It will be shown that for a wide class of symmetries SCRPA can be formulated in such a way that it also *maintains* these properties of standard RPA. This is to be considered as a strong advantage over other extensions of RPA because SCRPA, though much more demanding numerically than standard RPA, leads to an (nonlinear) equation of the Schrödinger type which seems to be accessible for a numerical solution. The restoration of symmetries within SCRPA is directly linked to the consideration of the so-called "scattering" terms and we will discuss their significance in detail.

Here we will demonstrate those properties of SCRPA in an exactly solvable three level Lipkin model [21, 22], which can also be interpreted as an interacting spin problem with two sites. Recently this model was investigated within the multistep variational approach [23] and the r-RPA formalism [24]. This model has the property that, as swon in Ref. [25], once the two upper levels become degenerate, a continuously broken symmetry develops beyond a certain critical coupling which can be considered as a deformed state with broken rotational symmetry. We will show that SCRPA, as standard RPA, will develop a zero mode (Goldstone mode) beyond a critical coupling, thus exactly restoring the original invariance of the Hamiltonian.

We also will see that SCRPA yields much improved solutions which we will compare with the ones obtained from an exact diagonalization. For the two particle case SCRPA even reproduces the exact results. In detail the paper is organized as follows. In Section 2 we give a short description of the SCRPA and emphasise the main differences with respect to r-RPA. We outline here and in the Appendix B the method to determine the one and two-body densities. In Section 3 we give some numerical examples

concerning especially the Goldstone mode. In Appendix A we describe a very efficient procedure to solve SCRPA as a system of coupled equations, based on r-RPA as a first step. In the last Section we draw our conclusions.

II. THEORETICAL BACKGROUND

Let us consider a many body system of fermions characterized by $n+1$ single particle levels, labelled $\alpha = 0, 1, 2, ..., n$. We define the "quadrupole-like" basis operators of this model

$$K_{\alpha\beta} \equiv \sum_{\mu=1}^{N} c^{\dagger}_{\alpha\mu} c_{\beta\mu} \ , \tag{2.1}$$

where $c^{\dagger}_{\alpha\mu}$ denotes the creation operator of a fermion on some α-th level. We suppose the levels degenerate, the total number of projections μ being $N = 2\Omega$. The operators (2.1) satisfy simple commutation rules, namely

$$[K_{\alpha\beta}, K_{\gamma\delta}] = \delta_{\beta\gamma} K_{\alpha\delta} - \delta_{\alpha\delta} K_{\gamma\beta} \ . \tag{2.2}$$

We will consider the following general Hamiltonian built on these operators

$$H = \sum_{\alpha=0}^{n} \epsilon_{\alpha} K_{\alpha\alpha} + \sum_{\alpha\beta\gamma\delta=0}^{n} V_{\alpha\beta\gamma\delta} K_{\alpha\beta} K_{\gamma\delta} \ . \tag{2.3}$$

We have chosen in our numerical application the three-level Lipkin model, with $n = 2$, corresponding to the SU(3) algebra. This model has been widely used in order to test different many-body approximations [21, 22, 23, 24, 25]. In analysing this model we have used a particular form of the Hamiltonian (2.3), namely

$$H = \sum_{\alpha=0}^{2} \epsilon_{\alpha} K_{\alpha\alpha} - \frac{V}{2} \sum_{\alpha=1}^{2} (K_{\alpha 0} K_{\alpha 0} + K_{0\alpha} K_{0\alpha}) \ . \tag{2.4}$$

It is a particular case of the Hamiltonian used in Ref. [26] and it is analyzed in detail in Ref. [25] in connection with a continuously broken symmetry which appears, as already mentioned, when $\epsilon_1 = \epsilon_2$.

We will analyze the SCRPA in order to obtain the excitation energies and we will compare the results with the r-RPA scheme as well as with the exact results, obtained by the diagonalization procedure.

We recall that both SCRPA and r-RPA schemes involve several common steps, namely [28]

A) One finds the minimum of generalised mean field equations coupled to the RPA fluctuations.

B) One determines the RPA eigenstates.

C) The RPA amplitudes are used to compute one and two-body correlated densities. At this step r-RPA supposes a factorisation for the two-body densities, while SCRPA uses a fully correlated approach.

The amplitudes are used to iterate the steps A, B and C until the convergency is achieved.

In the following we will shortly describe this procedure.

A. Mean field

As a first step in both SCRPA and r-RPA schemes we set up the generalised mean field equations. To this purpose let us introduce fermion creation operators in a general single particle basis as follows

$$a^{\dagger}_{k\mu} = \sum_{\alpha=0}^{n} C_{k\alpha} c^{\dagger}_{\alpha\mu} \ , \tag{2.5}$$

where the supposed real transformation matrix is orthogonal. The unity matrix for $C_{k\alpha}$ corresponds to a "spherical" minimum, while a non-diagonal transformation corresponds to a "deformed" one. According

to Ref. [25] for the three-level Lipkin model the above real matrix can be written as a product of two rotations, i.e.

$$\begin{aligned} C_{k\alpha} &= \begin{pmatrix} \cos\phi & \sin\phi & 0 \\ -\sin\phi & \cos\phi & 0 \\ 0 & 0 & 1 \end{pmatrix} \begin{pmatrix} 1 & 0 & 0 \\ 0 & \cos\psi & \sin\psi \\ 0 & -\sin\psi & \cos\psi \end{pmatrix} \\ &= \begin{pmatrix} \cos\phi & \sin\phi\cos\psi & \sin\phi\sin\psi \\ -\sin\phi & \cos\phi\cos\psi & \cos\phi\sin\psi \\ 0 & -\sin\psi & \cos\psi \end{pmatrix} . \end{aligned} \tag{2.6}$$

The basic operators (2.1) are replaced in this new basis by similar combinations of the new operators (2.5)

$$A_{ij} = \sum_{\mu=1}^{N} a^{\dagger}_{i\mu} a_{j\mu} . \tag{2.7}$$

By using the inverse transformation of (2.5) the Hamiltonian (2.3) takes the following form in the new basis

$$H = \sum_{ij=0}^{n} F_{ij} A_{ij} + \sum_{ijkl=0}^{n} G_{ijkl} A_{ij} A_{kl} , \tag{2.8}$$

where the coefficients are given respectively by

$$\begin{aligned} F_{ij} &= \sum_{\alpha=0}^{n} \epsilon_{\alpha} C_{i\alpha} C_{j\alpha} , \\ G_{ijkl} &= \sum_{\alpha\beta\gamma\delta=0}^{n} V_{\alpha\beta\gamma\delta} C_{i\alpha} C_{j\beta} C_{k\gamma} C_{l\delta} . \end{aligned} \tag{2.9}$$

The expectation value of the Hamiltonian (2.8) with the correlated vacuum $|0\rangle$ has the form

$$\mathcal{H} \equiv \langle 0|H|0\rangle = \sum_{ij=0}^{n} F_{ij} \langle ij\rangle + \sum_{ijkl=0}^{n} G_{ijkl} \langle ijkl\rangle , \tag{2.10}$$

where we introduced one and two-body densities as follows

$$\begin{aligned} \langle ij\rangle &\equiv \langle 0|A_{ij}|0\rangle , \\ \langle ijkl\rangle &\equiv \langle 0|A_{ij}A_{kl}|0\rangle . \end{aligned} \tag{2.11}$$

In order to derive the Mean Field (MF) equations let us now consider the following restricted functional

$$\mathcal{H}' = \mathcal{H} - \sum_{\alpha} E_{\alpha} \langle \alpha\alpha\rangle \sum_{k} C_{k\alpha} C_{k\alpha} . \tag{2.12}$$

We below will show that the terms with non-diagonal densities $\langle \alpha\beta\rangle$ vanish because they contain generators of the RPA basis, which can be inverted in terms of SCRPA annihilation phonons acting on the vacuum state. The extremum condition

$$\frac{\partial \mathcal{H}'}{\partial C_{n\alpha}} = 0 \tag{2.13}$$

leads to the following system of equations

$$\epsilon_{\alpha} \langle nn\rangle C_{n\alpha} + \sum_{jkl} \sum_{\beta\gamma\delta} (njkl;\alpha\beta\gamma\delta) C_{j\beta} C_{k\gamma} C_{l\delta} = E_n \langle nn\rangle C_{n\alpha} , \tag{2.14}$$

where we introduced as short-hand notation

$$(njkl;\alpha\beta\gamma\delta) \equiv \frac{1}{2} [\langle njkl\rangle V_{\alpha\beta\gamma\delta} + \langle jnkl\rangle V_{\beta\alpha\gamma\delta} + \langle kjnl\rangle V_{\gamma\beta\alpha\delta} + \langle ljkn\rangle V_{\delta\beta\gamma\alpha}] . \tag{2.15}$$

By inserting a formal summation $\sum_\mu \delta_{n\mu}$ and using the orthonormality condition for the MF amplitudes one obtains an eigenvalue problem

$$\sum_m H_{nm} C_{m\alpha} = E_\alpha \langle \alpha\alpha \rangle C_{n\alpha} \ . \tag{2.16}$$

We solve this system to determine the eigenvalues E_α and eigenvectors $C_{m\alpha}$ for $\alpha = 0, 1, ..., N$. In case we evaluate expectation values (2.10) using the standard HF vacuum one obtains what we shall call the "static minimum". If one uses the SCRPA correlated vacuum the result is called "dynamic minimum" (coupled with RPA fluctuations). In both cases the system (2.16) contains nonlinear relations, because the matrix H_{nm}

$$H_{nm} \ = \ \langle nn \rangle \sum_\mu \epsilon_\mu C_{n\mu} C_{m\mu} + \sum_{jkl} \sum_{\mu\beta\gamma\delta} (njkl; \mu\beta\gamma\delta) C_{m\mu} C_{j\beta} C_{k\gamma} C_{l\delta} \tag{2.17}$$

is written in terms of the eigenvectors and therefore it should be solved iteratively. For the "dynamic minimum" the iterative process is more complex because it involves the correlated vacuum, i.e. RPA amplitudes. As an initial solution we can consider the standard HF problem, leading to a decoupled form for the two-body matrix elements

$$\langle ijkl \rangle \approx \langle ii \rangle \langle kk \rangle \delta_{ij} \delta_{kl} + \langle ii \rangle (1 - \langle kk \rangle / N) \delta_{il} \delta_{jk} \ . \tag{2.18}$$

With $\langle ii \rangle \equiv \rho_i^{(0)} = \{1, 0\}$, one obtains directly from Eq. (2.14) the standard system of HF equations

$$\sum_m H_{nm}^{(0)} C_{m\alpha} = E_\alpha^{HF} C_{m\alpha} \ , \tag{2.19}$$

where $H_{nm}^{(0)}$ are the elements of the HF Hamiltonian, which we will give for a particular interaction considered in our numerical application. However, in general, it is not necessary to consider the $\langle kk \rangle$ in (2.18) as uncorrelated. With correlations included Eq. (2.18) will lead to the so-called renormalised RPA (r-RPA) (see below).

B. SCRPA equations

The procedure to derive the system of RPA equations is given in many textbooks, see e.g. [1, 5]. Here we will shortly recall the main steps in order to introduce the necessary notations. To this purpose we use the equation of motion technique. The SCRPA creation operators are defined by the following superposition of the basic pair generators

$$Q_\nu^\dagger = \sum_{m>i} (X_{mi}^\nu \delta Q_{mi}^\dagger - Y_{mi}^\nu \delta Q_{mi}) \ . \tag{2.20}$$

These operators are written in the MF basis as follows

$$\delta Q_{mi}^\dagger = N_{mi}^{-1/2} A_{mi}, \quad \delta Q_{mi} = \delta Q_{im}^\dagger = N_{mi}^{-1/2} A_{im} \ . \tag{2.21}$$

and define the excited states

$$|\nu\rangle = Q_\nu^\dagger |0\rangle \ . \tag{2.22}$$

The RPA annihilation operators define a vacuum state, i.e.

$$Q_\nu |0\rangle = 0 \ . \tag{2.23}$$

It is important to stress that we used the letters m and i not for labelling holes and particles, but only to remember the condition $m > i$ as written in (2.20). In this way we include in the basis all possible particle-hole (ph) and also the so called "scattering" elements with particle-particle (pp) and hole-hole (hh) configurations. This type of amplitudes is absent in standard RPA and we will have to discuss their significance in the course of the present paper. It has been recently shown that the inclusion of scattering terms allows to fulfil the energy weighted sum rule in the renormalised RPA (r-RPA) [27] and they may therefore be of importance.

The normalisation factor in (2.21) is given by the following mean value on the selfconsistent vacuum

$$\langle 0|[A_{im}, A_{nj}]|0\rangle = \delta_{mn}\delta_{ij}(\langle ii\rangle - \langle mm\rangle) \equiv \delta_{mn}\delta_{ij}N_{mi} \ . \tag{2.24}$$

We then evaluate the mean value of the double commutator between the Hamiltonian and the phonon operator (2.20) [28]. One obtains in this way the SCRPA system of equations

$$\begin{pmatrix} \mathcal{A} & \mathcal{B} \\ -\mathcal{B}^* & -\mathcal{A}^* \end{pmatrix} \begin{pmatrix} X^\nu \\ Y^\nu \end{pmatrix} = \omega_\nu \begin{pmatrix} X^\nu \\ Y^\nu \end{pmatrix} \ , \tag{2.25}$$

where the matrices are given by the well-known relations

$$\begin{aligned} \mathcal{A}_{mi,nj} &= \langle 0| \left[\delta Q_{mi}, \left[H, \delta Q^\dagger_{nj}\right]\right] |0\rangle \\ \mathcal{B}_{mi,nj} &= -\langle 0| \left[\delta Q_{mi}, [H, \delta Q_{nj}]\right] |0\rangle = -\mathcal{A}_{mi,jn} \ . \end{aligned} \tag{2.26}$$

Additionally we have the generalised mean field equations (2.13), which with (2.23) can also be written as

$$\langle 0|[H, Q_\nu]|0\rangle = \langle 0|[H, Q^\dagger_\nu]|0\rangle = \langle 0|[H, \delta Q^\dagger_\nu]|0\rangle = 0 \ . \tag{2.27}$$

The amplitudes satisfy usual normalisation and completeness conditions

$$\begin{aligned} \sum_{m>i} (X^\nu_{mi}X^\mu_{mi} - Y^\nu_{mi}X^\mu_{mi}) &= \delta_{\nu,\mu} \ , \\ \sum_\nu \left(X^\nu_{mi}X^\nu_{nj} - Y^\nu_{mi}X^\nu_{nj}\right) &= \delta_{mi,nj} \ . \end{aligned} \tag{2.28}$$

For the general Hamiltonian (2.8) one obtains the following form of the SCRPA matrices

$$\begin{aligned} a_{mi,nj} &\equiv N^{1/2}_{mi}N^{1/2}_{nj}\mathcal{A}_{mi,nj} \\ &= \frac{1}{2}(\delta_{ij}F_{mn} - \delta_{mn}F_{ji})(\langle ii\rangle + \langle jj\rangle - \langle mm\rangle - \langle nn\rangle) \\ &+ \sum_{ab}(G_{mabn}\langle iabj\rangle + G_{abmn}\langle abij\rangle)_S + \sum_{ab}(G_{aijb}\langle amnb\rangle + G_{abji}\langle abnm\rangle)_S \\ &- \sum_{ab}(G_{majb}\langle ianb\rangle + G_{aibn}\langle ambj\rangle)_S \ , \\ &- \frac{1}{2}\delta_{ij}\sum_{abc}(G_{abcn}\langle abcm\rangle + G_{abmd}\langle abnc\rangle)_S \\ &- \frac{1}{2}\delta_{mn}\sum_{abc}(G_{abci}\langle abcj\rangle + G_{abjc}\langle abic\rangle)_S \ , \\ b_{mi,nj} &= -a_{mi,jn} \ , \end{aligned} \tag{2.29}$$

where we used the following short-hand notation

$$(G_{ijkl}\langle abcd\rangle)_S \equiv G_{ijkl}\langle abcd\rangle + G_{klij}\langle cdab\rangle \ . \tag{2.30}$$

The r-RPA differs from the SCRPA procedure in the way to determine the two-body densities. By using the factorised ansatz (2.18) one obtains the r-RPA matrices

$$\begin{aligned} \mathcal{A}^{(0)}_{mi,nj} &= \frac{1}{2}(\delta_{ij}H^{(0)}_{mn} - \delta_{mn}H^{(0)}_{ji})(N^{1/2}_{mi}N^{-1/2}_{nj} + N^{-1/2}_{mi}N^{1/2}_{nj}) \\ &+ \left(\overline{G}_{mijn} - \frac{1}{N}\overline{G}_{jimn}\right) N^{1/2}_{mi}N^{1/2}_{nj} \\ \mathcal{B}^{(0)}_{mi,nj} &= \frac{1}{2}(\delta_{mj}H^{(0)}_{ni} - \delta_{in}H^{(0)}_{mj})(N^{1/2}_{mi}N^{-1/2}_{nj} - N^{-1/2}_{mi}N^{1/2}_{nj}) \\ &+ \left(\overline{G}_{minj} - \frac{1}{N}\overline{G}_{nimj}\right) N^{1/2}_{mi}N^{1/2}_{nj} \ , \end{aligned} \tag{2.31}$$

where we used the following notations

$$\overline{G}_{minj} = G_{minj} + G_{njmi} \ , \tag{2.32}$$

and

$$H^{(0)}_{mn} \equiv F_{mn} + \sum_a \left[G_{maan} + \left(\overline{G}_{aamn} - \frac{1}{N} \overline{G}_{maan} \right) \langle aa \rangle \right] \ . \tag{2.33}$$

With the help of the MF equation (2.19) one obtains that $H^{(0)}_{mn}$ is diagonal, i.e.

$$H^{(0)}_{mn} = \delta_{mn} E_n \ . \tag{2.34}$$

We should stress that the occupation numbers appearing in (2.33) are calculated, as will be explained later, with the correlated vacuum and therefore (2.34) is *not* equivalent to standard HF, even within the r-RPA scheme.

For r-RPA amplitudes with respect to the initial basis A_{mi}

$$x^{\nu}_{0,mi} \equiv N^{-1/2}_{mi} X^{\nu}_{0,mi} \ , \quad y^{\nu}_{0,mi} \equiv N^{-1/2}_{mi} Y^{\nu}_{0,mi} \ , \tag{2.35}$$

one obtains expressions with no phase space factors concerning the indices m, i, i.e. there appear no occupation numbers

$$\begin{aligned} x^{\nu}_{0,mi} &= \frac{1}{\omega^{(0)}_{\nu} - (E_m - E_i)} \sum_{nj} \left[\left(\overline{G}_{mijn} - \frac{1}{N} \overline{G}_{jimn} \right) \overline{X}^{\nu}_{0,nj} + \left(\overline{G}_{minj} - \frac{1}{N} \overline{G}_{nimj} \right) \overline{Y}^{\nu}_{0,nj} \right] \ , \\ y^{\nu}_{0,mi} &= \frac{-1}{\omega^{(0)}_{\nu} + (E_m - E_i)} \sum_{nj} \left[\left(\overline{G}_{mijn} - \frac{1}{N} \overline{G}_{jimn} \right) \overline{Y}^{\nu}_{0,nj} + \left(\overline{G}_{minj} - \frac{1}{N} \overline{G}_{nimj} \right) \overline{X}^{\nu}_{0,nj} \right] \ , \end{aligned} \tag{2.36}$$

where we defined the new amplitudes

$$\overline{X}^{\nu}_{0,mi} \equiv N_{mi} x^{\nu}_{0,mi} \ , \quad \overline{Y}^{\nu}_{0,mi} \equiv N_{mi} y^{\nu}_{0,mi} \ . \tag{2.37}$$

We mention here that the r-RPA amplitudes defined by Eqs. (2.35) and (2.37) are very important in solving numerically the SCRPA system of equations using the two-step method described in the Appendix A.

C. SCRPA densities

In order to estimate the expectation values of the one-body density operators within the SCRPA

$$\hat{\rho}_i \equiv \sum_{\mu} a^{\dagger}_{i\mu} a_{i\mu}, \quad i = 0, 1, 2 \ , \tag{2.38}$$

we need a special procedure. In the following we propose a method which is more convergent than the standard expansion in terms of phonon operators (2.20). To this purpose let us introduce the shell model basis, but in the MF representation and which do not necessarily correspond to the HF basis, as we see in (2.16)

$$|n_1 n_2\rangle \equiv \mathcal{N}^{-1/2}_{n_1 n_2} A^{n_1}_{10} A^{n_2}_{20} |MF\rangle, \quad 0 \leq n_1 + n_2 \leq N \ , \tag{2.39}$$

where $|MF\rangle$ corresponds to a Slater determinant built with operators (2.5). Within this complete basis we can expand a general combination of one-body densities

$$\begin{aligned} \hat{\rho}^{k_0}_0 \hat{\rho}^{k_1}_1 \hat{\rho}^{k_2}_2 &= \sum_{n_1 n_1 = 0}^{N} b_{n_1 n_2}(k_0 k_1 k_2) |n_1 n_2\rangle\langle n_2 n_1| \\ &= \sum_{n_1 n_1 = 0}^{N} c_{n_1 n_2}(k_0 k_1 k_2) A^{n_1}_{10} A^{n_2}_{20} A^{n_2}_{02} A^{n_1}_{01} \ , \end{aligned} \tag{2.40}$$

where k_0, k_1, k_2 are some given exponents. The connection between the b and c coefficients is given by iterating the resolution of the unity. This method is used in Ref. [30] and [31] . For us it is important to find the coefficients $c_{n_1 n_2}(k_0 k_1 k_2)$ and we will use a more direct technique. To this purpose we need the expectation values of the operators (2.40) on the correlated vacuum $|0\rangle$. They are calculated by using the inversion of (2.20). One obtains

$$\begin{aligned} A_{mi} &= N_{mi}^{1/2} \sum_\nu (X_{mi}^\nu Q_\nu^\dagger + Y_{mi}^\nu Q_\nu) \ , \\ A_{im} &= N_{mi}^{1/2} \sum_\nu (X_{mi}^\nu Q_\nu + Y_{mi}^\nu Q_\nu^\dagger) \ , \end{aligned} \tag{2.41}$$

where the normalisation factor N_{mi} is given by (2.24). For instance in the case of products of two operators one obtains the following relations for $m > i, n > j$

$$\begin{aligned} \langle 0|A_{mi}A_{nj}|0\rangle &= N_{mi}^{1/2} N_{nj}^{1/2} \sum_\nu Y_{mi}^\nu X_{nj}^\nu \\ \langle 0|A_{im}A_{jn}|0\rangle &= N_{mi}^{1/2} N_{nj}^{1/2} \sum_\nu X_{mi}^\nu Y_{nj}^\nu \\ \langle 0|A_{mi}A_{jn}|0\rangle &= N_{mi}^{1/2} N_{nj}^{1/2} \sum_\nu Y_{mi}^\nu Y_{nj}^\nu \\ \langle 0|A_{im}A_{nj}|0\rangle &= N_{mi}^{1/2} N_{nj}^{1/2} \sum_\nu X_{mi}^\nu X_{nj}^\nu \ . \end{aligned} \tag{2.42}$$

We mention that these relations can be directly used to express some of the SCRPA matrix elements in terms of RPA amplitudes. One finally obtains from (2.40) a nonlinear system of equations, determining the normalisation factors N_{10}, N_{20}. It is given in the Appendix B in terms of expansion coefficients defined by Eq. (2.40). These coefficients are fast decreasing with increasing $n_1 + n_2$. One can see from the Table 2 that already the linear approximation, i.e. $n_1 + n_2 \leq 1$, ensures an accuracy of the order 10^{-2}. In this case one also directly obtains the one-body densities

$$\begin{aligned} \langle 0|\hat{\rho}_m|0\rangle &= \left[y_{mm} + \frac{y_{11}y_{22}}{N}\right] \left[1 + \frac{2}{N}(y_{11}+y_{22}) + \frac{3}{N^2} y_{11}y_{22}\right]^{-1} , \quad m = 1, 2 \ , \\ \langle 0|\hat{\rho}_0|0\rangle &= N - \langle 0|\hat{\rho}_1|0\rangle - \langle 0|\hat{\rho}_2|0\rangle \ , \end{aligned} \tag{2.43}$$

where

$$y_{mn} = \sum_\nu Y_{m0}^\nu Y_{n0}^\nu \ . \tag{2.44}$$

Based on this result one may hope that also for a more realistic $n+1$-level model one can expand the product of densities in the ph "shell-model" basis, i.e.

$$|n_1 n_2 ... n_n\rangle \equiv \mathcal{N}_{n_1 n_2 ... n_n}^{-1/2} A_{10}^{n_1} A_{20}^{n_2} ... A_{n0}^{n_n} |0\rangle, \quad 0 \leq n_1 + n_2 + ... + n_n \leq 1 \ . \tag{2.45}$$

III. NUMERICAL APPLICATION

A. Hartree-Fock mean field

In order to apply the SCRPA and r-RPA procedures it is convenient to start iterations using standard HF and RPA solutions. To this purpose let us first evaluate the expectation values of the one and two-body operators on the standard HF vacuum

$$\begin{aligned} \langle \alpha\beta\rangle &= \delta_{\alpha\beta}\delta_{\alpha 0} N \ , \\ \langle \alpha\beta\gamma\delta\rangle &= \delta_{\alpha 0}\delta_{\delta 0}\delta_{\beta\gamma} N \left[1 + \delta_{\beta 0}(N-1)\right] \ . \end{aligned} \tag{3.1}$$

We stress that the two-body density has the same form as the factorised ansatz (2.18). The expectation value of the Hamiltonian (2.4) then becomes

$$\begin{aligned} \langle H\rangle &= F_{00}N + \sum_\alpha G_{0\alpha\alpha 0} N + G_{0000} N(N-1) \\ &= N\epsilon[e_0 \cos^2\phi + e_1 \sin^2\phi\cos^2\psi + e_2 \sin^2\phi\sin^2\psi \\ &- \chi \sin^2\phi\cos^2\phi] \ , \end{aligned} \tag{3.2}$$

where we introduced the following dimensionless notations

$$e_k = \frac{\epsilon_k}{\epsilon}, \quad \chi = \frac{V(N-1)}{\epsilon} \ . \tag{3.3}$$

The Hamiltonian (2.4) has two kinds of HF minima, namely a spherical minimum and a deformed one

$$\begin{aligned} &1) \quad \phi = 0, \quad \psi = 0 \ , \quad \chi < e_1 - e_0 \ , \\ &2) \quad \cos 2\phi = \frac{e_1 - e_0}{\chi}, \quad \psi = 0, \quad \chi > e_1 - e_0 \ . \end{aligned} \tag{3.4}$$

Moreover, our calculations have shown that for any MF minimum one obtains $\psi = 0$, defined by the parametrisation (2.6), independent of which kind of vacuum (correlated or not) we use to estimate the expectation values.

B. Standard RPA

For the above mentioned minima we obtain that the standard RPA matrix elements have very simple expressions. By using the following short-hand notation for the index pairs

$$10 \to 1, \ 20 \to 2, \ 21 \to 3 \tag{3.5}$$

one obtains [25]

$$\begin{aligned} \mathcal{A}_{11} &= \epsilon(e_1 - e_0)\cos\,2\phi + \epsilon\frac{3}{2}\chi\sin^2\,2\phi \ , \\ \mathcal{A}_{22} &= \epsilon(e_2 - e_0\cos^2\phi - e_1\sin^2\phi) + \epsilon\frac{1}{2}\chi\sin^2 2\phi \ , \\ \mathcal{A}_{12} &= \mathcal{A}_{21} = 0 \ , \\ \mathcal{B}_{11} &= -\epsilon\chi(\cos^4\phi + \sin^4\phi) \ , \\ \mathcal{B}_{22} &= -\epsilon\chi\cos^2\phi \ , \\ \mathcal{B}_{12} &= \mathcal{B}_{21} = 0 \ . \end{aligned} \tag{3.6}$$

Therefore the $\mathcal{A}$ and $\mathcal{B}$ RPA matrices are diagonal. The RPA frequencies are easy to estimate

$$\omega_k^2 = \mathcal{A}_{kk}^2 - \mathcal{B}_{kk}^2 \ , \quad k = 1, 2 \ , \tag{3.7}$$

and the amplitudes become

$$\begin{pmatrix} X_k^\nu \\ Y_k^\nu \end{pmatrix} = \frac{1}{\sqrt{2}}\left[\frac{\mathcal{A}_{kk}}{\omega_k} \pm 1\right]^{1/2} \delta_{k\nu} \tag{3.8}$$

We fix the origin of the particle spectrum with $e_0 = 0$. Then for a spherical vacuum $\phi = 0$ the RPA energies are given by

$$\omega_\nu = \epsilon_\nu \left[1 - \left(\frac{\chi}{e_\nu}\right)^2\right]^{1/2} \ , \quad \nu = 1, 2 \ , \tag{3.9}$$

with the corresponding RPA amplitudes

$$\begin{pmatrix} X_k^\nu \\ Y_k^\nu \end{pmatrix} = \frac{1}{\sqrt{2}}\left[\frac{\epsilon_k}{\omega_k} \pm 1\right]^{1/2} \delta_{k\nu} \ . \tag{3.10}$$

As it was shown in Ref. [25], if the upper single particle levels are degenerate, i.e. $\Delta\epsilon \equiv \epsilon_2 - \epsilon_1 = 0$, for the values of the strength $\chi > e_1$, in the "deformed region", i.e. with $\phi \neq 0$ given by HF minimum, one obtains a Goldstone mode. In this case by considering $e_1 = 1$ one obtains for the excitation energies

$$\begin{aligned} \omega_1 &= \epsilon\sqrt{2(\chi^2 - 1)} \ , \\ \omega_2 &= 0 \ . \end{aligned} \tag{3.11}$$

Indeed, in Fig. 1 by dashed lines are plotted standard RPA excitation energies versus the strength parameter χ, by considering the number of particles $N = 10$. For $\chi < 1$ (spherical region) the eigenvalues ω_1, ω_2 are degenerate, while for $\chi > 1$ (deformed region, $\phi \neq 0$) the second mode ω_2 has a vanishing value, i.e. it corresponds to the Goldstone mode. In this case the amplitude of the non-vanishing mode are given by

$$\begin{pmatrix} X_1^1 \\ Y_1^1 \end{pmatrix} = \frac{1}{\sqrt{2}} \left(\frac{3\chi - 1/\chi}{2\sqrt{2(\chi^2 - 1)}} \pm 1 \right) \ , \quad X_2^1 = Y_2^1 = 0 \ . \tag{3.12}$$

The corresponding amplitudes for the Goldstone mode are given by

$$X_1^2 = Y_1^2 = 0 \ , \quad X_2^2 = Y_2^2 \to \infty \ . \tag{3.13}$$

A similar plot for $N = 20$ is given in Fig. 2.

C. SCRPA for N=2

It is possible to find the exact eigenstates of the three-level Lipkin Hamiltonian (2.4) by diagonalizing it in the following normalized basis

$$|n_1 n_2\rangle = \sqrt{\frac{(N - n_1 - n_2)!}{N! n_1! n_2!}} K_{10}^{n_1} K_{20}^{n_2} |HF\rangle \ . \tag{3.14}$$

In this paragraph we will pay special attention to the spherical case $\phi = 0$, with $N = 2$, i.e. the two-particle case. The above diagonalisation basis contains 6 elements with $n_1 + n_2 \leq 2$. The calculation shows that the non-vanishing components of the ground state are $|n_1 n_2\rangle = |00\rangle, |20\rangle, |02\rangle$. The first two excited states contain only $|10\rangle$ and $|01\rangle$ components, respectively. This fact suggests that we can consider the two component phonon, with components $(10) \to 1, (20) \to 2$. The corresponding SCRPA vacuum state has the following form

$$|0\rangle = \left(a_0 + \frac{a_1}{2} K_{10}^2 + \frac{a_2}{2} K_{20}^2 \right) |MF\rangle \ . \tag{3.15}$$

By using the action of the annihilation operator on the vacuum (2.23) one obtains for the coefficients

$$\begin{aligned} a_0 &= \left[1 + \left(YX^{-1} \right)_{11}^2 + \left(YX^{-1} \right)_{22}^2 \right]^{-1/2} \ , \\ a_1 &= a_0 \left(YX^{-1} \right)_{11} \ , \\ a_2 &= a_0 \left(YX^{-1} \right)_{22} \ . \end{aligned} \tag{3.16}$$

The one-body densities and their products can be expressed in terms of the vacuum amplitudes as follows

$$\begin{aligned} \langle 0|\hat{\rho}_k|0\rangle &= 2a_k^2 \ , \quad \langle 0|\hat{\rho}_k^2|0\rangle = 4a_k^2 \ , \quad k = 0, 1, 2 \ , \\ \langle 0|\hat{\rho}_0 \hat{\rho}_1|0\rangle &= \langle 0|\hat{\rho}_0 \hat{\rho}_2|0\rangle = \langle 0|\hat{\rho}_1 \hat{\rho}_2|0\rangle = 0 \ . \end{aligned} \tag{3.17}$$

The SCRPA matrix elements of the Hamiltonian (2.4) can be directly evaluated by computing double commutators expectation values with respect to the vacuum. It turns out that they are diagonal and therefore the two eigenstates are decoupled. This allows us to express in a simple way the coefficients entering the vaccuum state

$$z_k \equiv \left(YX^{-1} \right)_{kk} = \frac{Y_k}{X_k} \ , \quad k = 1, 2 \ . \tag{3.18}$$

The SCRPA matrix elements have the following form

$$\begin{aligned}
\mathcal{A}_{11} &= \epsilon\left[e_1 - e_0 + \chi\frac{2z_1+z_2}{1-z_1^2}\right] , \\
\mathcal{A}_{22} &= \epsilon\left[e_2 - e_0 + \chi\frac{2z_2+z_1}{1-z_2^2}\right] , \\
\mathcal{A}_{12} &= \mathcal{A}_{21} = 0 , \\
\mathcal{B}_{11} &= -\epsilon\chi\frac{1+z_1^2+z_1z_2}{1-z_1^2} , \\
\mathcal{B}_{22} &= -\epsilon\chi\frac{1+z_2^2+z_2z_1}{1-z_2^2} , \\
\mathcal{B}_{12} &= \mathcal{B}_{21} = 0 .
\end{aligned} \tag{3.19}$$

The matrix elements of the Hamiltonian with respect to the above vacuum give the ground state energy as follows

$$E_0 = 2\epsilon\frac{e_1z_1^2 + e_2z_2^2 - \chi(z_1+z_2)}{1+z_1^2+z_2^2} . \tag{3.20}$$

The SCRPA equations lead to the following nonlinear system of equations for z_1, z_2

$$\begin{aligned}
\frac{\chi}{2e_1}\left[z_1^4 - 2z_1^2 + \left(z_1^3 - z_1\right)z_2 + 1\right] + z_1^3 - z_1 &= 0 , \\
\frac{\chi}{2e_2}\left[z_2^4 - 2z_2^2 + \left(z_2^3 - z_2\right)z_1 + 1\right] + z_2^3 - z_2 &= 0 .
\end{aligned} \tag{3.21}$$

We solved this system by using the Newton procedure with a precision of 10^{-8}. The results for both eigenvalues and amplitudes coincide with the exact values using the diagonalisation procedure, independent of the used coupling constant χ and single particle energies. In Table 1 we give the coefficients $a_k, k = 0, 1, 2$, the ground state energy and the excitation energies $\omega_k, k = 1, 2$ for $\chi = 5,\ e_0 = 0,\ e_1 = 1,\ e_2 = 2,\ \epsilon = 1\ MeV$. The two lines correspond both to the exact and SCRPA values and they fully coincide. Therefore it is possible to construct the SCRPA ground state and excitations, which actually coincide with the exact solution. The inclusion of the third component (21) in the structure of the vacuum state for $N = 2$ gives a vanishing coefficient and therefore it is not necessary to consider it in this case.

Table 1

The vacuum coefficients $a_k, k = 0, 1, 2$ in (3.15), the ground state energy and the excitation energies $\omega_k, k = 1, 2$ at $\chi = 5,\ \epsilon_n = n\ MeV,\ n = 0, 1, 2$ for the exact and SCRPA values.

	a_0	a_1	a_2	E_0	ω_1	ω_2
exact	0.772576	0.496911	0.395228	-5.773794	6.773794	7.773794
SCRPA	0.772576	0.496911	0.395228	-5.773794	6.773794	7.773794

For $N > 2$ the equation (2.23) leads to a system where the number of conditions exceeds the number of coefficients. In order to find the SCRPA ground state by satisfying the condition (2.23) it is necessary to enlarge the basis, by considering e.g. for $N = 4$ two particle-two hole(2p-2h) excitations together with the (21) component. Recently similar conclusions were obtained for the many level pairing model in Ref. [10].

As a matter of fact it is easy to convince one self that SCRPA is able to give the exact solution of any two-body problem. The ground state of a general two particle system can be written as

$$|0\rangle \sim \left(1 + \frac{1}{4}\sum_{p_1h_1p_2h_2} z_{p_1h_1p_2h_2}a^\dagger_{p_1}a_{h_1}a^\dagger_{p_2}a_{h_2}\right)|MF\rangle , \tag{3.22}$$

where the 2p-2h coefficients obey the following symmetry relations

$$z_{p_1h_1p_2h_2} = -z_{p_1h_2p_2h_1} = -z_{p_2h_1p_1h_2} = z_{p_2h_2p_1h_1} . \tag{3.23}$$

Applying the vacuum condition (2.23) on this state one obtains

$$\sum_{ph}\left(-Y_{ph}^{\nu *}+\sum_{p'h'}z_{php'h'}X_{p'h'}^{\nu *}\right)a_p^\dagger a_h|MF\rangle=0\ , \tag{3.24}$$

or

$$Y_{ph}^{\nu *}\ =\ \sum_{p'h'}z_{php'h'}X_{p'h'}^{\nu *}\quad \text{for all } \nu\ , \tag{3.25}$$

which implies that

$$z_{php'h'}\ =\ \left[YX^{-1}\right]^*_{php'h'}\ . \tag{3.26}$$

Since we have now expressed the exact ground state in terms of the SCRPA amplitudes, we also can deduce that the SCRPA excitation energies are the exact ones because the RPA destruction operator can be written as $Q_\nu=|0\rangle\langle\nu|$, where $|\nu\rangle$ are the exact state vectors of the two particle excited states. On the other hand $Q_\nu^\dagger=|\nu\rangle\langle 0|$ fulfils exactly the SCRPA equation of motion (2.25). We therefore see that SCRPA solves a general two particle problem exactly as long as one can define a Fermi surface. This, however, should in principle always be possible in putting the two particle system in an external box potential with or without periodic boundary conditions and solve the SCRPA equations in the limit of an infinitely large box.

D. SCRPA in the spherical region

Let us first discuss the SCRPA results in the spherical region, i.e. the region where the generalised mean field equation (2.14) has only the trivial solution $\phi=0$. In comparison with standard HF this region is strongly extended. The content of the spherical region depends on the particle number. We have seen that for $N=2$ the spherical region covers all values of χ, since we obtained the exact solution. For $N=10$ or $N=20$ the spherical region is typically extended by a factor of two. This comes from the selfconsistent coupling of the quantal fluctuations to the mean field.

Let us now consider the definite example $e_0=0,\ e_1=1,\ e_2=2$ for $N=20$. In Fig. 3 we show by dashed lines the SCRPA results for the excitation energies, compared with the exact ones (solid lines) and to standard RPA (dot-dashes). We see that SCRPA strongly improves over standard RPA and in fact first and second excited states are excellently reproduced up to χ-values of about $\chi\approx 1.2$. The third state has no analogue in standard RPA and must therefore be attributed to the scattering configuration (21). The SCRPA solution for the the third eigenvalue definitely seems to approximate the fifth exact eigenvalue in the range $0\le\chi\le 1.0$. The fifth eigenvalue has mainly a 2p-2h structure and it seems natural that the inclusion of scattering terms allows to reproduce such states, since e.g. $a_p^\dagger a_{p'}$ in a boson expansion picture is represented by a 2p-2h configuration, i.e.

$$a_p^\dagger a_{p'}\approx\sum_h B_{ph}^\dagger B_{p'h}\ , \tag{3.27}$$

where B_{ph} are ideal boson operators (see [5], Ch. 9). The fact that SCRPA, via the scattering terms, is able to describe states of the 2p-2h type is very satisfying and in a way astonishing. Indeed the single particle energy differences which correspond to the $a_p^\dagger a_{p'}$ configuration are $e_p-e_{p'}$ and in our example this gives $e_2-e_1=1$. One should have thought that for $\chi\to 0$ the third eigenvalue goes to one. In fact it can be shown that for χ strictly zero, the third eigenvalue *is* one. However, this is a singular point and for any finite value of χ the third SCRPA root jumps to the values shown in Fig. 3. A closer inspection reveals that this latter feature is entirely due to the genuine two-body correlations contained in SCRPA, because in the r-RPA the third eigenvalue is completely modified and indeed stays close to $e_2-e_1=1$. We repeated the calculation for $\Delta\epsilon=e_2-e_1=0.001$. In Fig. 4 for $N=10$ and Fig. 5 for $N=20$ we see that the scenario concerning the third eigenvalue stays practically unchanged and, therefore, this seems to be a quite robust feature. In Fig. 6 we show the r-RPA solution for the $\Delta\epsilon=0.001$ case. Indeed there, in the spherical region, a very low-lying third eigenvalue appears which is of the order $\Delta\epsilon$ and thus not distinguishable from the abscissa on the scale of the figure. We therefore see that the genuine two-body correlations have dramatic effect in order to restore the situation for the third eigenvalue.

It is also interesting to investigate the influence of the scattering terms on the other SCRPA eigenvalues. We therefore performed the calculation switching off the (21)-component in the SCRPA equations for $N = 10$ case. In Table 2 we give the results. It is seen that the influence of the scattering terms on the first and second SCRPA eigenvalues is very weak.

Table 2

The eigenvalues for the two-dimensional $\omega_k^{(2)},\ k = 1, 2$ and three dimensional $\omega_k^{(3)},\ k = 1, 2, 3$ versions of the SCRPA versus the strength χ (first column) in the spherical region. The particle number is $N = 10$ and $\epsilon_n = n\ MeV,\ n = 0, 1, 2$. In the columns 2-4 are given the exact solutions $\omega_k\ , k = 1, 2, 5$. In the last columns are given ground state energies for two-dimensional and three-dimensional SCRPA and exact values, respectively.

χ	ω_1	ω_2	ω_5	$\omega_1^{(2)}$	$\omega_2^{(2)}$	$\omega_1^{(3)}$	$\omega_2^{(3)}$	$\omega_3^{(3)}$	$E_0^{(2)}$	$E_0^{(3)}$	$E_0^{(exact)}$
0.900	0.745	1.758	2.888	0.774	1.908	0.778	1.910	3.102	-0.407	-0.409	-0.354
0.920	0.735	1.752	2.887	0.767	1.905	0.772	1.907	3.106	-0.427	-0.429	-0.371
0.940	0.726	1.745	2.886	0.761	1.902	0.766	1.904	3.111	-0.447	-0.450	-0.388
0.960	0.716	1.739	2.886	0.755	1.899	0.760	1.901	3.116	-0.468	-0.470	-0.406
0.980	0.706	1.733	2.885	0.749	1.896	0.754	1.898	3.122	-0.490	-0.492	-0.423
1.000	0.696	1.727	2.885	0.744	1.893	0.749	1.895	3.128	-0.512	-0.514	-0.442
1.020	0.686	1.722	2.885	0.738	1.889	0.744	1.891	3.135	-0.534	-0.536	-0.461
1.040	0.677	1.717	2.886	0.733	1.886	0.739	1.888	3.143	-0.557	-0.559	-0.480
1.060	0.667	1.712	2.886	0.728	1.883	0.734	1.885	3.151	-0.580	-0.582	-0.500
1.080	0.657	1.707	2.887	0.723	1.880	0.729	1.882	3.160	-0.604	-0.606	-0.520
1.100	0.647	1.703	2.889	0.719	1.877	0.725	1.879	3.169	-0.628	-0.631	-0.540

In Figs. 7 and 8 we show the SCRPA groundstate energies for $N = 10$ and $N = 20$, respectively as a function of the angle ϕ representing the mean field transformation. We take $\Delta\epsilon = 0.001$. We see that for a large plateau of χ-values the minimum stays at $\chi = 0$. This region is more or less enhanced by a factor of two, compared with standard HF theory, where the $\phi = 0$ minimum ceases to exist at $\chi = 1$. In SCRPA, after the $\phi = 0$ solution is finished, the system jumps in a discontinuous manner to the "new" deformed solution. This discontinuity is clearly seen in Figs. 9 ($N = 10$) and 10 ($N = 20$) where we show the ground state energy $E_0^{(SCRPA)}$ (dashed line) and compare it with the exact values (solid line) and standard RPA (dot-dashed line). The full 3x3 SCRPA with the scattering terms was used. We see a strong improvement of SCRPA versus standard RPA in the transition region where standard HF switches from the spherical to deformed regime. Beyond this transition point SCRPA stays spherical and slightly overbinds whereas standard RPA goes deformed and slightly underbinds. From the point where also SCRPA jumps to the deformed solution, standard and SCRPA give almost identical correlation energies.

E. SCRPA in the deformed region

In the deformed region a particular situation arises in our model for $\Delta\epsilon = 0$, since, as already mentioned, a spontaneously broken symmetry occurs in this case. Here the standard HF-RPA exhibits its real strength because, as shown in (3.11), a zero mode appears which signifies that the broken symmetry is restored, i.e. the conservation laws are fulfilled [1, 5]. We will now demonstrate that this property is conserved in SCRPA (with scattering terms). In this context we mention that the symmetry operator

$$\hat{L}_0 = i(K_{21} - K_{12}) = i\left[A_{20} - A_{02})\sin\phi + (A_{21} - A_{12})\cos\phi\right]\ , \tag{3.28}$$

which commutes with the Hamiltonian, can be identified with the z-component of the rotation operator. This operator contains scattering terms which are, however, also present in our RPA-ansatz and therefore we can expect that (3.28) is a particular RPA operator with a zero eigenvalue solution in SCRPA, very much in the same way as this is the case in standard RPA. The numerical verification of this desirable quality of SCRPA must however be undertaken with care. Indeed, a zero mode contains diverging amplitudes which, injected into the SCRPA matrix, may not lead to selfconsistency. The way to overcome

this difficulty is to start the calculation with a finite small value of $\Delta\epsilon$, i.e. with a slight explicit symmetry breaking, and then to diminish its value step by step. We, in this way, could verify with very high accuracy that the zero eigenvalue occurs in the deformed region for all values of the interaction strength χ. This is shown in Fig. 4 by a solid line for $N = 10$ and Fig. 5 for $N = 20$. Here we considered the value $\Delta\epsilon = 0.001$, but we were able to reach the value $\Delta\epsilon = 10^{-6}$.

In spite of this clear appearance of the Goldstone mode, which only shows up when scattering terms are included and the generalised mean field equation (2.14) is solved selfconsistently with the SCRPA equations, the spectrum in the deformed region needs some discussion and clarification. First of all one notices a discontinuity when passing from the spherical to the deformed region. This feature of deformed SCRPA has been already noticed earlier with other models: the two level Lipkin model [28] and the two level pairing model [29]. It is reminiscent of a first order phase transition which, however, is absent in the exact solution.

Furthermore the second SCRPA eigenvalue seems too low compared with the exact solution and also, astonishingly, with respect to the standard RPA solution, as seen in Figs. 1,2. In fact standard RPA works surprisingly well in the deformed region, a fact which seems to be a constancy in all the models we have investigated so far [28, 29].

Third, in the deformed region it does not seem easy to identify the third SCRPA eigenvalue with any of the exact solutions. Therefore, in spite of satisfying the Goldstone theorem, the interpretation of SCRPA seems less clear in the deformed region than it appears in the spherical one. However, the situation may be less unsatisfactory than it appears at first sight.

As usual with a continuously broken symmetry also in the present model a clear rotational band structure is revealed, as can be seen by inspecting Figs. 1,2. The exact solution, found by a diagonalisation procedure, has a definite angular momentum projection L_0. Moreover the expectation value of the L_0^2 operator has integer values, namely

$$\sqrt{\langle L_0^2 \rangle} = J = 0, 1, 2, ... \tag{3.29}$$

The first "rotational band" $J = 0, 1, 2, ...$ is built on top of the RPA excitation with a vanishing energy (Goldstone mode). The second "band-head" corresponds to the second RPA mode (dashed curve) and the corresponding members of this "excited band" have a different slope with respect to the "ground band". On the same figures one can also see a third "rotational band".

As customary in RPA theory one also can evaluate the mass parameter of the rotational band within SCRPA. By a straightforward generalisation we obtain for the moment of inertia (see e.g. Ref. [1, 5])

$$M = 2L_0^* \left(\mathcal{A} - \mathcal{B}\right)^{-1} L_0 \ , \tag{3.30}$$

where $\mathcal{A}, \mathcal{B}$ are the SCRPA matrices and L_0 denotes the part with $m > i$ components of the momentum operator (3.28), which should be written in terms of normalised generators $\delta Q^\dagger$ defined by Eq. (2.21), i.e.

$$L_0 = i \left(0, \ N_{20}^{1/2} sin\phi, \ N_{21}^{1/2} cos\phi\right) \ . \tag{3.31}$$

For the standard RPA case, by using the matrix elements given by (3.6), and $N_{20} = N$, one obtains an analytical solution, namely

$$M = \frac{N(\chi - 1)}{\epsilon\chi(\chi + 1)} \ . \tag{3.32}$$

In Fig. 11 we show by a solid line the above moment of inertia calculated with RPA for $N = 20$ and in Fig. 12 with SCRPA. The comparison with the "exact" mass parameter fitted from the exact spectrum is also given by dashed curves. From the dot-dashed lines, giving their ratio, we see that the SCRPA mass is slightly closer to the "exact" value than the corresponding RPA value. This is also manifest when comparing the rotational energies, as in Fig. 13. Here we plotted by dashes the SCRPA spectrum and by solid lines the "exact" values.

One therefore sees that one can recover rather clearly the precise position of the lowest energy value and therefore the discontinuity, at least of the first excited state, in crossing the phase boundary, is much less pronounced, than the one which is seen in Figs. 4, 5. One may think that the same upward shift should also be observed for the second SCRPA eigenvalue (the band head of the second rotational band) bringing it in a close agreement with the exact solution. It then appears that one can use SCRPA with scattering terms in the same way as standard RPA with all usual properties conserved. Let us mention

that even in r-RPA the Goldstone mode appears when the scattering terms are considered. This is shown in Fig. 6. Note, however, that in the spherical region the third r-RPA eigenvalue also comes almost zero value. The reason for this was discussed above.

F. The occupation numbers

The reproduction of energies may not be the most sensitive indicator for the performance of a theory. Usually wavefunctions are much more demanding in this respect. We therefore calculated for $\Delta\epsilon = 0.001$ the occupation numbers which reflect more directly the quality of the wave function, since they are not obtained from a minimisation procedure, as the energies.

In Figs. 14, 15 we show the SCRPA results for $\langle 0|\rho_0|0\rangle$, $\langle 0|\rho_1|0\rangle$ and $\langle 0|\rho_2|0\rangle$ according to Eq. (2.43). We see that in the spherical region the SCRPA densities (solid lines) are rather close to the exact values (dashes) for χ-values up to slightly above one. This is, of course, much better than standard RPA (not shown) which breaks down, as the energies, well before $\chi = 1$, but the region $1 \leq \chi \leq 2$ remains not well reproduced. On the contrary in the deformed region the SCRPA results are excellent. It is somewhat unexpected to see that the occupation numbers of the two upper but degenerated levels are not equal but their averaged sum very well reproduce the exact occupancy of the two upper levels (dotted lines in Figs. 14, 15). Therefore the SCRPA wavefunction performs well in the deformed region.

IV. CONCLUSIONS

In this paper we studied various aspects of the SCRPA in the three level Lipkin model. With respect to the two level Lipkin model, the three level version has the advantage of allowing for a continuously broken symmetry on the mean field level with the appearance of a Goldstone mode. One major objective of the present work therefore was to investigate whether in SCRPA the very desirable properties of standard RPA concerning exact restoration of symmetry and fullfillment of conservation laws can also be maintained. We found out that this is indeed the case under the condition that the symmetry operator is fully included in the RPA operator as a particular solution. In our model this implies that the RPA operator contains in addition to the usual ph and hp components $a_p^\dagger a_h$ and $a_h^\dagger a_p$ also the so-called anomalous or scattering terms $a_p^\dagger a_{p'}$ and $a_h^\dagger a_{h'}$.

With a correlated ground state the inclusion of such terms is perfectly possible since the occupation numbers are now different from one and/or zero and mathematically the situation becomes similar to the finite temperature RPA case, where also pp' and hh' components are allowed. However, it was found in this work that the inclusion of such scattering terms is not without problem. For example pp' (hh') configurations can imply very small energy differences $\epsilon_p - \epsilon_{p'} \approx 0$ and therefore for small interaction very low-lying roots may be found in the spectrum which are absent in the exact solution. In our model it turned out that this is the case only in the approximate, so-called renormalised version of SCRPA. On the contrary, in the full SCRPA the eigenvalue which is linked to the inclusion of scattering terms corresponds to a 2p-2h state of the exact spectrum. This is true in the "spherical" region whereas in the symmetry broken phase the third eigenvalue does not seem to have any precise correspondent in the exact solution. In the symmetry unbroken phase the elimination of the anomalous terms has an insignificant influence on the reminder of the spectrum. In the symmetry broken phase this inclusion is crucial to produce the Goldstone mode at zero energy, otherwise this state is pushed up to quite high energy with no equivalent in the exact spectrum. We also calculated the moment of inertia of the rotational band which works in SCRPA (with scattering terms) in a way very analogous to standard RPA. Very good agreement with the exact solution is found. Therefore the present formulation of SCRPA allows to maintain all the formal and desirable properties of standard RPA. There is only one unpleasant feature which is that SCRPA solutions do not join smoothly when passing from the symmetry unbroken to the symmetry broken phase. Whether this can be improved upon remains to be seen in future work. A further very attractive feature of SCRPA is the fact that it solves any two body problem *exactly*. This is contrary to the usual where many body approximations deteriorate when decreasing the number of particles.

Quite remarkably the SCRPA solution exists in the symmetry unbroken single particle basis well beyond the phase transition point given by the standard RPA and the excited state is well approximated in all this region. For $N = 10$ and $N = 20$ at a certain strength $\overline{\chi}_{crt} \approx 2\chi_{crt}$, where χ_{crt} is the value where standard HF becomes unstable, SCRPA also jumps to the deformed solution. A similar behaviour of SCRPA has already been found for other models.

Though the appearance of the Goldstone mode is a very desirable feature, since this signals that conservation laws and sum rules are fulfilled, it turned out that in the deformed region, contrary to the "spherical" one, the SCRPA only very slightly improves over standard RPA and both, SCRPA and standard RPA are quite close to the exact solution. Again this is a feature which also has been found in other models. It seems that the common wisdom that "deformation" sums already a lot of additional correlations in standard RPA is born out here.

We therefore can summarize the studies of SCRPA in various models in the following way: in the symmetry unbroken regime SCRPA works excellently, yielding simultaneously very good ground state and excitation energies. One can work in the spherical basis beyond the usual transition point given by the instability of the standard HF solution. This "beyond" depends on the number of particles and the model. SCRPA solves a general two particle system *exactly*.

In the deformed region SCRPA does not seem to improve very much over standard "deformed" RPA. However, all formal properties of standard RPA are maintained with SCRPA when the scattering terms are included. For example for nuclei SCRPA will give a Goldstone mode restoring translational invariance. The transition from "spherical" to "deformed" is discontinuous, which is an unpleasant feature. It is not evident that the inclusion of scattering components in the *spherical region* improves the results. It also should be mentioned that the appearance of the Goldstone mode in SCRPA is only guaranteed when the symmetry operator does not contain any diagonal components as $a_i^\dagger a_i$, since those terms cannot be included in the RPA operator. Such a situation occurs for example in the case of particle number violation [5].

Acknowledgements

One of us (D.S.D.) is grateful for the financial support given by IPN Orsay, were part the work was performed. J.D. gratefully acknowledges partial support by the Spanish DGI under Grant BFM2003-05316-C02-02. Discussions with M. Sambataro, M.Grasso (Catania) and N.V. Giai (Orsay) are gratefully acknowledged.

Appendix A
SCRPA in two steps

The SCRPA system of equations (2.25) and the normalisation condition for amplitudes can be written in a matrix form respectively as follows

$$\begin{aligned} \mathcal{S}\mathcal{X} &= \overline{\mathcal{X}}\Omega \ , \\ \mathcal{X}^{\dagger}\overline{\mathcal{X}} &= \mathcal{I} \ . \end{aligned} \tag{A.1}$$

Here we introduced some short-hand notations

$$\begin{aligned} \mathcal{S} = \begin{pmatrix} a & b \\ b^* & a^* \end{pmatrix} \ , \quad \mathcal{X} = \begin{pmatrix} x & y^* \\ y & x^* \end{pmatrix} \ , \quad \overline{\mathcal{X}} = \mathcal{N}\mathcal{X} \ , \\ \mathcal{N} = \begin{pmatrix} N & 0 \\ 0 & -N \end{pmatrix} \ , \quad \mathcal{I} = \begin{pmatrix} I & 0 \\ 0 & -I \end{pmatrix} \ , \quad \Omega = \begin{pmatrix} \omega & 0 \\ 0 & -\omega \end{pmatrix} \ . \end{aligned} \tag{A.2}$$

Here the matrices $a,\ b$ are defined by Eq. (2.29). We used the amplitudes $\mathcal{X}$ relative to the initial generators A_{mi} defined by Eq. (2.35) and also the SCRPA matrices defined by Eq. (2.29). We also introduced similar to (2.37) amplitudes $\overline{\mathcal{X}}$. N is the diagonal metric matrix $N_k\delta_{kl}$, where we used for the basis indices the notation $(mi) \to k$

$$(10) \to 1, \quad (20) \to 2, \quad (21) \to 3 \ . \tag{A.3}$$

SCRPA equations are written as

$$\mathcal{N}\overline{\mathcal{S}\mathcal{X}} = \overline{\mathcal{X}}\Omega \ , \tag{A.4}$$

in terms of the SCRPA matrix relative to $\overline{\mathcal{X}}$ amplitudes

$$\overline{\mathcal{S}} = \mathcal{N}^{-1}\mathcal{S}\mathcal{N}^{-1} \ . \tag{A.5}$$

From the normalisation condition one derives the inverse amplitude matrix

$$\mathcal{X}^{-1} = \mathcal{I}\overline{\mathcal{X}}^{\dagger} \ , \tag{A.6}$$

giving the following resolution of the unity

$$\mathcal{X}\mathcal{I}\overline{\mathcal{X}}^{\dagger} = \mathbf{I} \equiv \begin{pmatrix} I & 0 \\ 0 & I \end{pmatrix} \ . \tag{A.7}$$

Let us split the SCRPA matrix into two parts: the r-RPA matrix plus a fluctuation

$$\mathcal{S} = \mathcal{S}_0 + \delta\mathcal{S} \ , \tag{A.8}$$

where $\delta\mathcal{S} = \mathcal{S} - \mathcal{S}_0$. The r-RPA system of equations and the normalisation condition are given by

$$\begin{aligned} \mathcal{S}_0\mathcal{X}_0 &= \overline{\mathcal{X}}_0\Omega_0 \ , \\ \mathcal{X}_0^{\dagger}\overline{\mathcal{X}}_0 &= \mathcal{I} \ , \\ \overline{\mathcal{X}}_0 &= \mathcal{N}\mathcal{X}_0 \ . \end{aligned} \tag{A.9}$$

We should stress on the important fact that our calculation is selfconsistent because we use the SCRPA set of amplitudes in deriving the metric matrix $\mathcal{N}$ in the r-RPA system of equations. We insert the unity operator written in terms of r-RPA amplitudes

$$\mathcal{X}_0\mathcal{I}\overline{\mathcal{X}}_0^{\dagger} = \mathbf{I} \ , \tag{A.10}$$

in front of $\mathcal{X}$ amplitudes of the left hand side Eq. (A.1). By using r-RPA equations (A.9) one gets

$$\left(\overline{\mathcal{X}}_0\Omega_0 + \delta\mathcal{S}\mathcal{X}_0\right)\mathcal{I}\mathcal{X}_0^{\dagger}\overline{\mathcal{X}} = \overline{\mathcal{X}}\Omega \ . \tag{A.11}$$

We multiply this relation to the left with $\overline{\mathcal{X}}_0^{-1} = \mathcal{I}\mathcal{X}_0^\dagger$. One finally obtains a standard system of RPA equations

$$(\Omega_0\mathcal{I} + \delta\mathcal{S}')\,\mathcal{X}' = \mathcal{I}\mathcal{X}'\Omega \ , \tag{A.12}$$

with the normalisation condition for new amplitudes

$$\mathcal{X}'^\dagger\mathcal{I}\mathcal{X}' \ = \ \mathcal{I} \ , \tag{A.13}$$

where

$$\begin{aligned} \mathcal{X}' \ &= \ \mathcal{X}_0^\dagger\overline{\mathcal{X}} \ , \\ \delta\mathcal{S}' \ &= \ \mathcal{I}\mathcal{X}_0^\dagger\delta\mathcal{S}\mathcal{X}_0\mathcal{I} \ . \end{aligned} \tag{A.14}$$

In particular one has

$$\begin{aligned} \delta a' \ &= \ x_0^\dagger\delta a x_0 + x_0^\dagger\delta b y_0 + y_0^\dagger\delta b x_0 + y_0^\dagger\delta a y_0 \ , \\ \delta b' \ &= \ -x_0^\dagger\delta a y_0 - x_0^\dagger\delta b x_0 - y_0^\dagger\delta b y_0 - y_0^\dagger\delta a x_0 \ . \end{aligned} \tag{A.15}$$

This is an RPA system of equations with r-RPA energies on the diagonal. It corresponds to a new representation of the SCRPA phonon

$$Q_\nu^\dagger = \sum_\alpha \left(x_\alpha'^\nu Q_{0\alpha}^\dagger - y_\alpha'^\nu Q_{0\alpha} \right) \ , \tag{A.16}$$

in terms of r-RPA phonons

$$Q_{0\alpha}^\dagger = \sum_{m>i} \left(x_{0k}^\alpha A_{mi} - y_{0k}^\alpha A_{im} \right) \ . \tag{A.17}$$

The formulation of SCRPA, where the division by the norm matrix $\mathcal{N}$ has disappeared, has the important formal aspect that one sees that the division by eventual very small numbers or even zero, contained in $\mathcal{N}$, in reality does not exists. This is also born out by our three component SCRPA solution treated in the main text.

Appendix B
Operator expansion method for densities

In order to find the coefficients of the expansion (2.40) it is possible to use the resolution of unity method [30, 31]. We proceed in a more direct way by computing the matrix elements with respect the complete basis (2.39). One obtains a lower triangular system of equations

$$\sum_{n_1 \leq m_1} \sum_{n_2 \leq m_2} \mathcal{M}^{n_1 n_2}_{m_1 m_2} c_{n_1 n_2}(k_0 k_1 k_2) = \mathcal{L}_{m_1 m_2}(k_0 k_1 k_2) \ , \tag{B.1}$$

where

$$\begin{aligned} \mathcal{M}^{n_1 n_2}_{m_1 m_2} &\equiv \mathcal{N}^{-1}_{m_1 m_2} \langle 0 | A^{m_2}_{02} A^{m_1}_{01} A^{n_1}_{10} A^{n_2}_{20} A^{n_2}_{02} A^{n_1}_{01} A^{m_1}_{10} A^{m_2}_{20} | 0 \rangle \ , \\ \mathcal{L}_{m_1 m_2}(k_0 k_1 k_2) &\equiv \mathcal{N}^{-1}_{m_1 m_2} \langle 0 | A^{m_2}_{02} A^{m_1}_{01} \hat{\rho}^{k_0}_0 \hat{\rho}^{k_1}_1 \hat{\rho}^{k_2}_2 A^{m_1}_{10} A^{m_2}_{20} | 0 \rangle \ . \end{aligned} \tag{B.2}$$

The solution of this system is given by the following recurrent relation

$$c_{m_1 m_2}(k_0 k_1 k_2) = \frac{1}{\mathcal{M}^{m_1 m_2}_{m_1 m_2}} \left[\mathcal{L}_{m_1 m_2}(k_0 k_1 k_2) - \sum_{n_1 n_2 < m_1 m_2} \mathcal{M}^{n_1 n_2}_{m_1 m_2} c_{n_1 n_2}(k_0 k_1 k_2) \right] \ . \tag{B.3}$$

Let us consider the HF ansatz of the vacuum, defined by

$$a^\dagger_{i\mu} a_{j\nu} | HF \rangle = \delta_{ij} \delta_{\mu\nu} \delta_{i0} | HF \rangle \ . \tag{B.4}$$

The coefficients of the system (B.1) are given in a straightforward way

$$\begin{aligned} \mathcal{L}_{m_1 m_2}(k_0 k_1 k_2) &= (N - m_1 - m_2)^{k_0} m_1^{k_1} m_2^{k_2} \\ \mathcal{M}^{n_1 n_2}_{m_1 m_2} &= \mathcal{N}_{m_1 m_2} \frac{(N - m_1 - m_2 + n_1 + n_2)!}{N! (m_1 - n_1)! (m_2 - n_2)!} \\ \mathcal{N}_{m_1 m_2} &= \frac{N! m_1! m_2!}{(N - m_1 - m_2)!} \\ c_{00}(k_0 k_1 k_2) &= N^{k_0} \delta_{k_1 0} \delta_{k_2 0} \ . \end{aligned} \tag{B.5}$$

We give the solutions of this system for $n_1 + n_2 \leq 2$

$$\begin{aligned} \hat{\rho}^k_0 &\approx N^k + \frac{(N-1)^k - N^k}{N} (A_{10} A_{01} + A_{20} A_{02}) \\ &+ \frac{1}{2N(N-1)} \left[(N-2)^k + N^{k-1}(N-2) - \frac{2(N-1)^{k+1}}{N} \right] \\ &\times (A^2_{10} A^2_{01} + A^2_{20} A^2_{02} + 2 A_{10} A_{20} A_{02} A_{01}) \\ \hat{\rho}^k_m &\approx \frac{1}{N} A_{m0} A_{0m} + \frac{1}{N(N-1)} \left[(2^{k-1} - 1 + \frac{1}{N}) A^2_{m0} A^2_{0m} + \frac{1}{N} A_{10} A_{20} A_{02} A_{01} \right] \\ \hat{\rho}_0 \hat{\rho}_m &\approx \frac{N-1}{N} A_{m0} A_{0m} - \frac{1}{N^2(N-1)} (A^2_{m0} A^2_{0m} + A_{10} A_{20} A_{02} A_{01}) \\ \hat{\rho}_1 \hat{\rho}_2 &\approx \frac{1}{N(N-1)} A_{10} A_{20} A_{02} A_{01} \ , \end{aligned} \tag{B.6}$$

where $m = 1, 2$. These expansions are very convergent. Indeed, this can be seen in Table 3, where there are given the expansion coefficients $c_{n_1 n_2}(k_0 k_1 k_2)$ with $n_1 + n_2 \leq 2$ for $N = 10$.

In order to find the normalisation factors N_{i0} using the expansion (2.40) up to $n_1 + n_2 \leq 2$ we need the expectation values for the following products of operators

$$\begin{aligned} \langle 0 | A_{m0} A_{0m} | 0 \rangle &= N_{m0} \sum_\nu Y^\nu_{m0} Y^\nu_{m0} \\ &\equiv N_{m0} y_{mm} \ , \\ \langle 0 | A_{m0} A_{n0} A_{0n} A_{0m} | 0 \rangle &= N_{m0} N_{n0} \sum_{\nu\mu} [Y^\nu_{m0} Y^\mu_{m0} X^\nu_{n0} X^\mu_{n0} \\ &+ Y^\nu_{m0} Y^\nu_{m0} Y^\mu_{n0} Y^\mu_{n0} + Y^\nu_{m0} Y^\mu_{m0} Y^\nu_{n0} Y^\mu_{n0}] \\ &\equiv N_{m0} N_{m0} z_{mn} \ . \end{aligned} \tag{B.7}$$

For $n_1 + n_2 \leq 2$ one obtains the following system in terms of the expansion coefficients in Eq. (2.40)

$$\begin{aligned} N_{10} &= c_{00}(100) - c_{00}(010) + [c_{10}(100) - c_{10}(010)]N_{10}y_{11} + [c_{01}(100) - c_{01}(010)]N_{20}y_{22} \\ &+ [c_{20}(100) - c_{20}(010)]N_{10}^2 z_{11} + [c_{02}(100) - c_{02}(010)]N_{20}^2 z_{22} \\ &+ [c_{11}(100) - c_{11}(010)]N_{10}N_{20}z_{12} \ , \\ N_{20} &= c_{00}(100) - c_{00}(001) + [c_{10}(100) - c_{10}(001)]N_{10}y_{11} + [c_{01}(100) - c_{01}(001)]N_{20}y_{22} \\ &+ [c_{20}(100) - c_{20}(001)]N_{10}^2 z_{11} + [c_{02}(100) - c_{02}(001)]N_{20}^2 z_{22} \\ &+ [c_{11}(100) - c_{11}(001)]N_{10}N_{20}z_{12} \ . \end{aligned} \tag{B.8}$$

Table 3

The expansion coefficients $c_{n_1 n_2}(k_0 k_1 k_2)$ in Eq. (2.40) with $n_1 + n_2 \leq 2$ for $N = 10$.

n_1, n_2 / k_1, k_2, k_3	0,0	0,1	1,0	0,2	1,1	2,0
1,0,0	10.0000	-0.1000	-0.1000	-0.0011	-0.0022	-0.0011
0,1,0	0.0000	0.0000	0.1000	0.0000	0.0011	0.0011
0,0,1	0.0000	0.1000	0.0000	0.0011	0.0011	0.0000
2,0,0	100.0000	-1.9000	-1.9000	-0.0100	-0.0200	-0.0100
0,2,0	0.0000	0.0000	0.1000	0.0000	0.0011	0.0122
0,0,2	0.0000	0.1000	0.0000	0.0122	0.0011	0.0000
1,1,0	0.0000	0.0000	0.9000	0.0000	-0.0011	-0.0011
0,1,1	0.0000	0.0000	0.0000	0.0000	0.0111	0.0000
1,0,1	0.0000	0.9000	0.0000	-0.0011	-0.0011	0.0000

[1] J.P.Blaizot and G. Ripka, *Quantum Theory of Finite Systems* (MIT Press, Cambridge, 1986).
[2] G.D. Mahan, *Many Particle Physics* (Plenum Press, New York, 1981).
[3] J.W. Negele, H. Orland, *Quantum Many Particle Systems, Frontiers in Physics* (Addison Weseley, New York, 1988).
[4] A.L. Fetter and J.D. Walecka, *Quantum Theory of Many particle Systems* (McGraw-Hill, New York, 1971).
[5] P. Ring and P. Schuck, *The Nuclear Many-Body Problem* (Springer Verlag, New York, 1980).
[6] C.J. Pethick, H. Smith, *Bose-Einstein Condensation in Dilute Gases* (Cambridge University Press, 2002).
[7] L. Pitaevski and S. Stringari, *Bose-Einstein Condensation, International Series of Monographs on Physics* (Clarendon Press, Oxford, 2003).
[8] F. Catara, G. Piccitto, M. Sambataro, and N. Van Giai, Phys. Rev. **B54**, 17536 (1996); F. Catara, M. Grasso, G. Piccitto, and M. Sambataro, Phys. Rev. **B58**, 16070 (1998).
[9] G. Baym and L.P. Kadanoff, Phys. Rev. **124**, 287 (1961); G. Baym, Phys. Rev. **127**, 1391 (1962); G. Baym, Phys. Lett. **1**, 242 (1962).
[10] J.G. Hirsch, A. Mariano, J. Dukelsky, and P. Schuck, Ann. Phys. (NY) **296**, 187 (2002).
[11] K. Hara, Progr. Theor. Phys. **32**, 88 (1964).
[12] D.J. Rowe, Rev. Mod. Phys. **40**, 153 (1968).
[13] D.J. Rowe, Phys. Rev. **175**, 1283 (1968).
[14] J. Toivanen and J. Suhonen, Phys. Rev. Lett. **75**, 410 (1995).
[15] J. Suhonen et al., Z. Phys. **A358**, 358 (1997).
[16] A.A. Raduta et al., Nucl. Phys. **A634**, 497 (1998).
[17] J. Dukelsky, G. Röpke, and P.Schuck, Nucl. Phys. **A628**, 17 (1998).
[18] G. Röpke, Z. Phys. **B99**, 83 (1995) and the references therein.
[19] A. Storozhenko, P. Schuck, J. Dukelsky, G. Röpke, and A. Vdovin, Ann. Phys. (NY) **307**, 308 (2003).
[20] P. Krüger and P. Schuck, Europhys. Lett. **27**, 395 (1994).
[21] S.Y. Li, A. Klein and R.M. Dreizler, J. Math. Phys. **11**, 975 (1970).
[22] N. Meshkov, Phys. Rev. **C3**, 2214 (1971).
[23] M. Sambataro, Phys. Rev. **C60**, 064320 (1999).
[24] M. Grasso, F. Catara, and M. Sambataro, Phys. Rev. C **66**, 064303 (2002).
[25] K. Hagino and G.F. Bertsch, Phys. Rev. **C61**, 024307 (2000).
[26] G. Holzwarth and T. Yukawa, Nucl. Phys. **A219**, 125 (1974).
[27] M. Grasso and F. Catara, Phys. Rev. **C63**, 014317 (2001).
[28] J. Dukelsky and P. Schuck, Nucl. Phys. **A512**, 466 (1990).
[29] A. Rabhi, R. Bennaceur, G. Chanfray, and P. Schuck, Phys. Rev. C **66**, 064315 (2002).
[30] G. Schalow and M. Yamamura, Nucl. Phys. **A161**, 93 (1971).
[31] B. Feucht, Université J. Fourier de Grenoble, Maìtrise de Physique, Institut de Physique Nucléaire, Juin 2000.

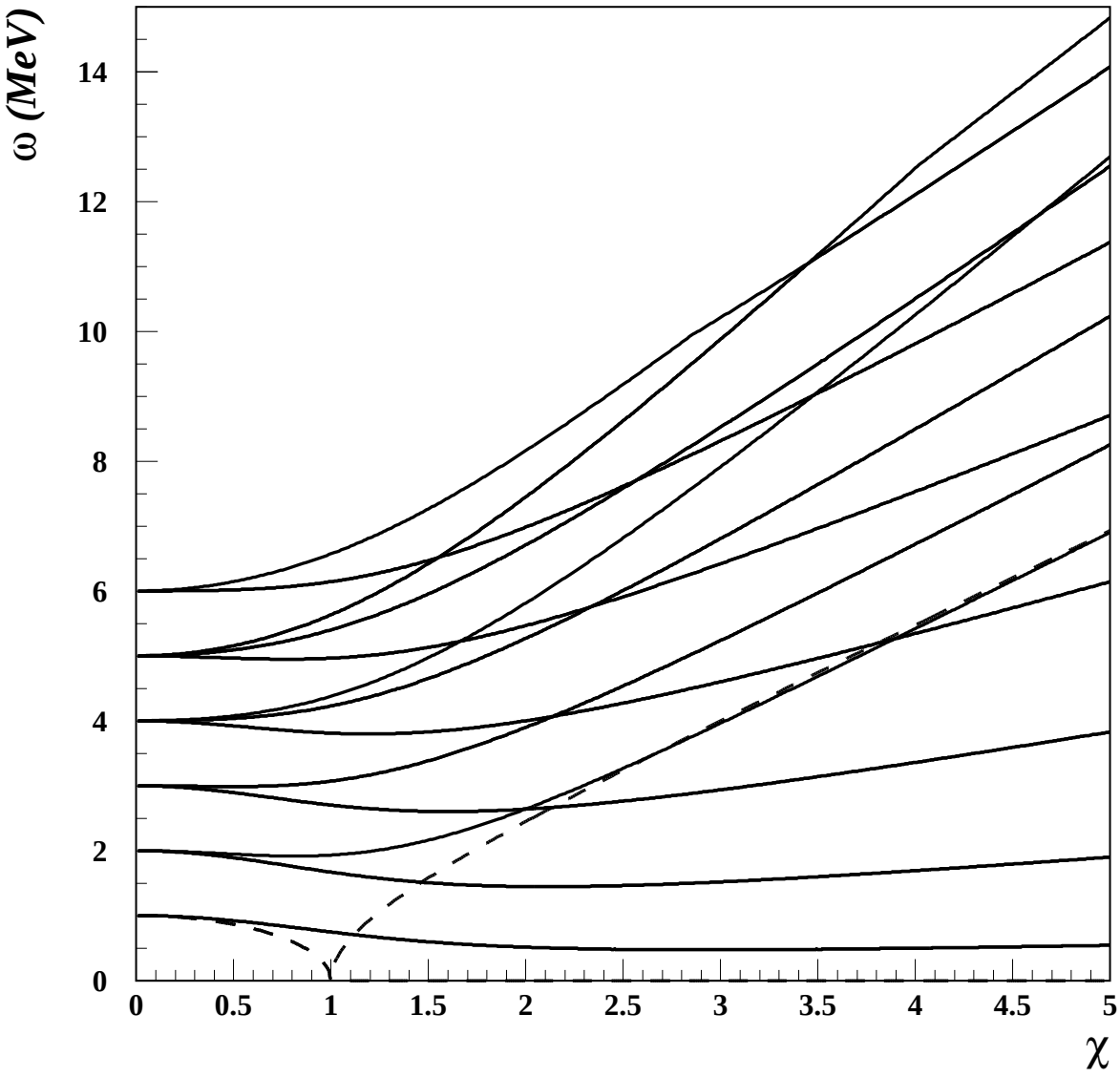

FIG. 1: Exact excitation energies versus the strength parameter χ, for $N = 10$, $\epsilon_1 = 0, \epsilon_2 = \epsilon_3 = 1MeV$. By dashes are given standard RPA values. Notice the appearance of a zero mode solution (Goldstone mode) beyond χ=1.

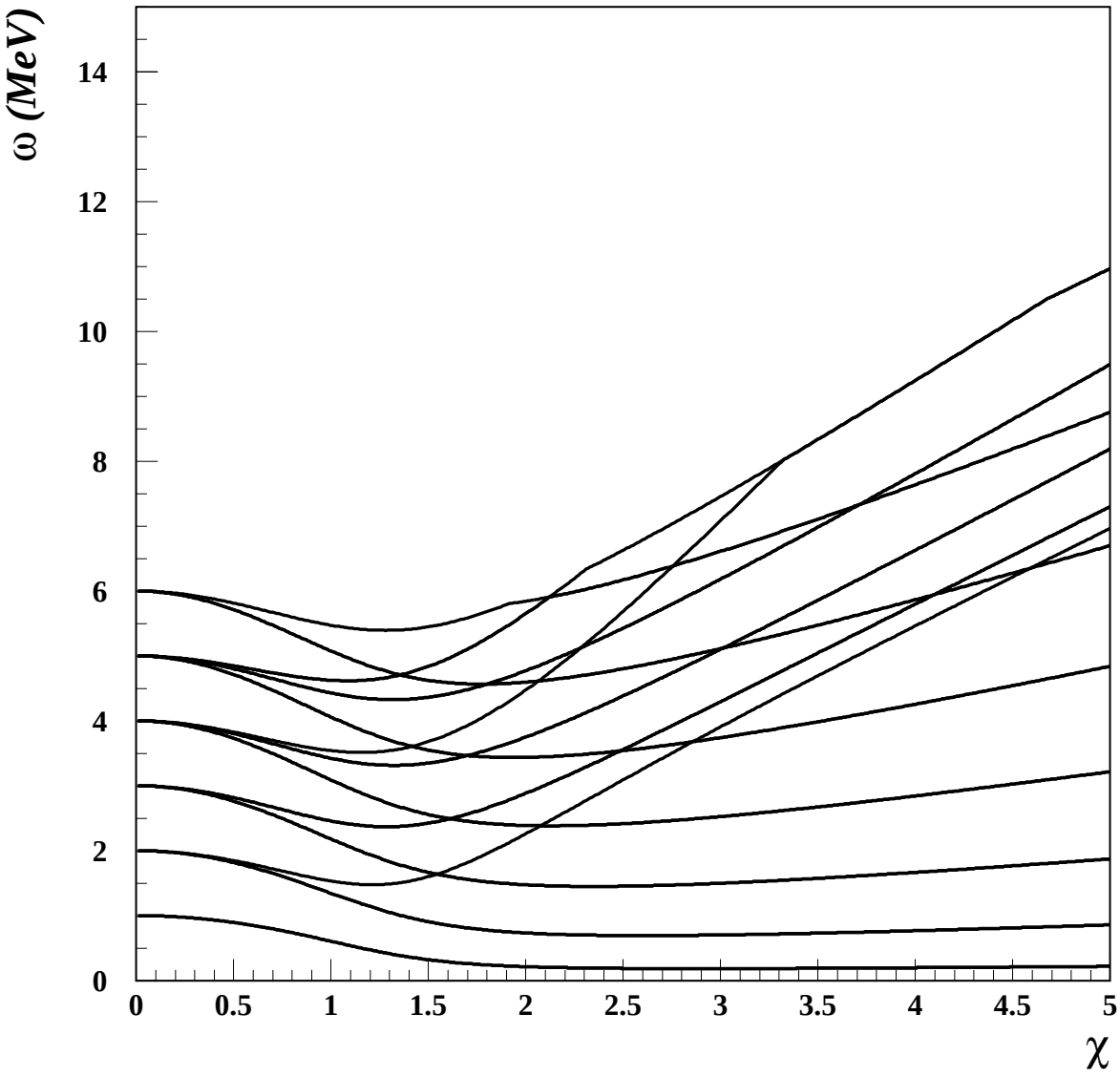

FIG. 2: The same as in Fig. 1, but for $N = 20$.

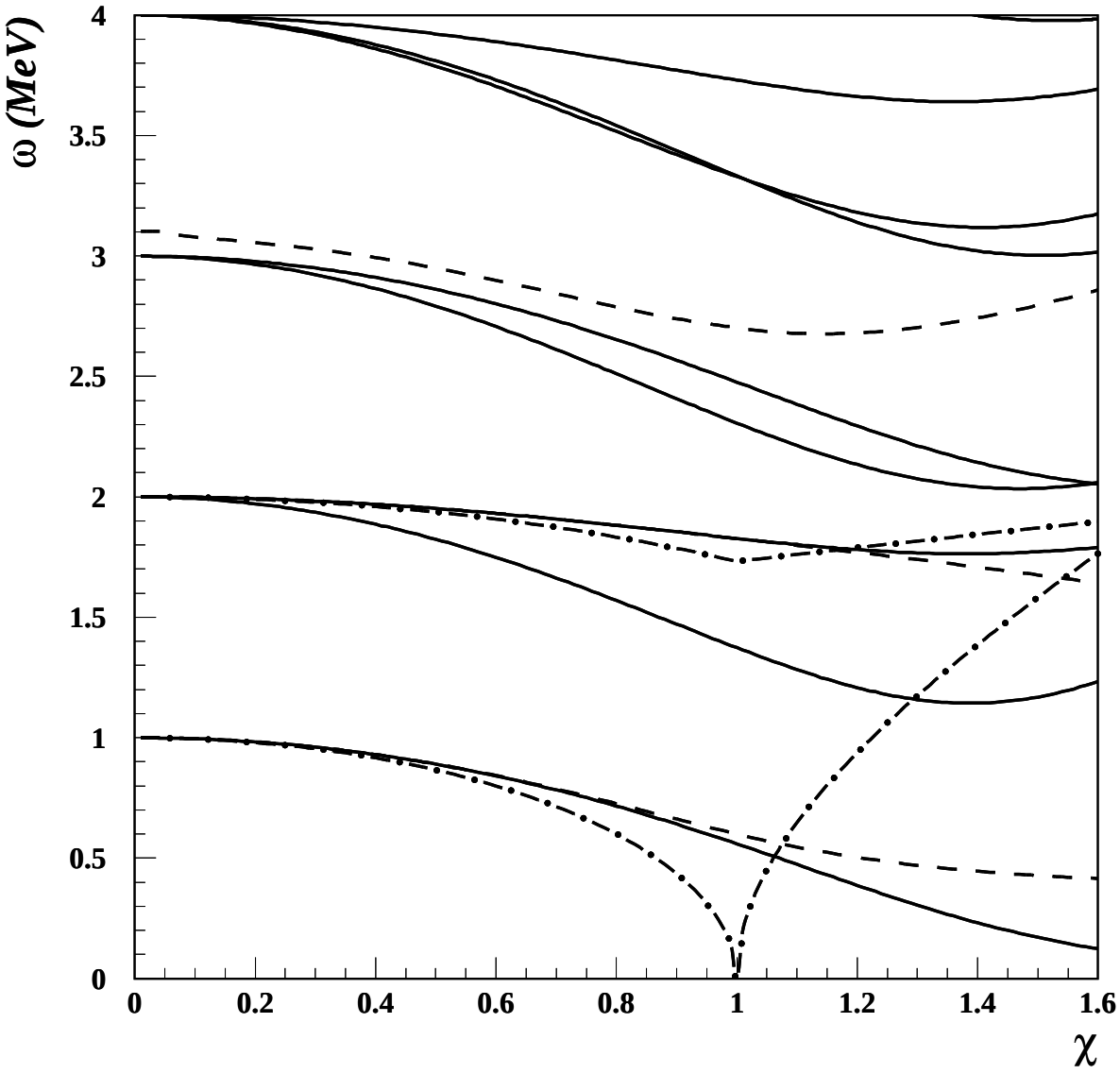

FIG. 3: SCRPA excitation energies versus the strength parameter χ, for $N = 20$ and $e_0 = 0,\ e_1 = 1,\ e_2 = 2$ (dashed lines). By solid lines are given the lowest exact eigenvalues and by dot-dashes the standard RPA energies.

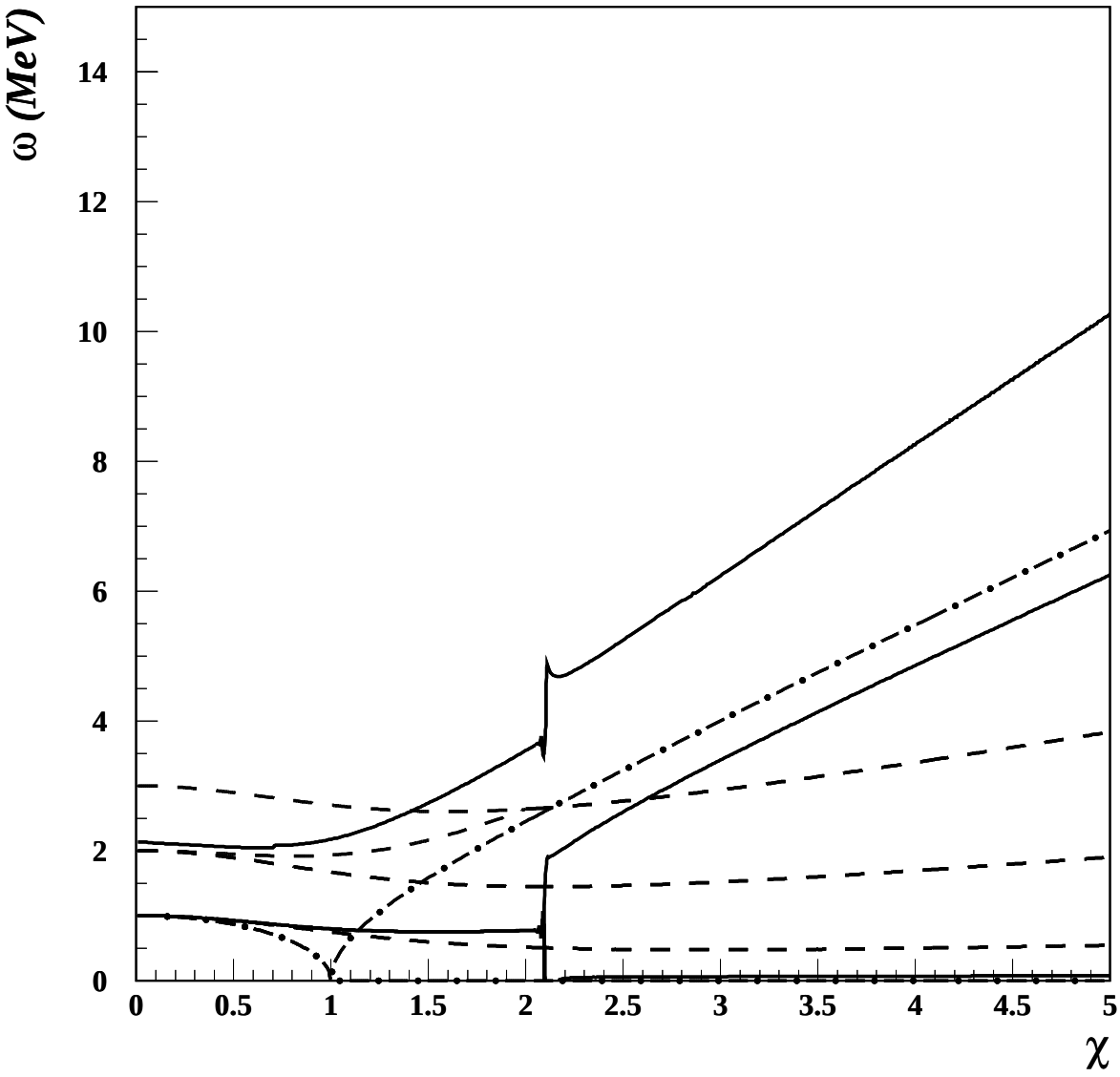

FIG. 4: SCRPA excitation energies versus the strength parameter χ, for $N = 10$, $\Delta\epsilon = 0.001\ MeV$ (full line). By dashes are given the lowest exact eigenvalues and by dot-dashes the standard RPA energies. After the phase transition point $\chi = 1$ (standard RPA) and $\chi \approx 2.1$ (SCRPA) a Goldstone mode at zero energy appears.

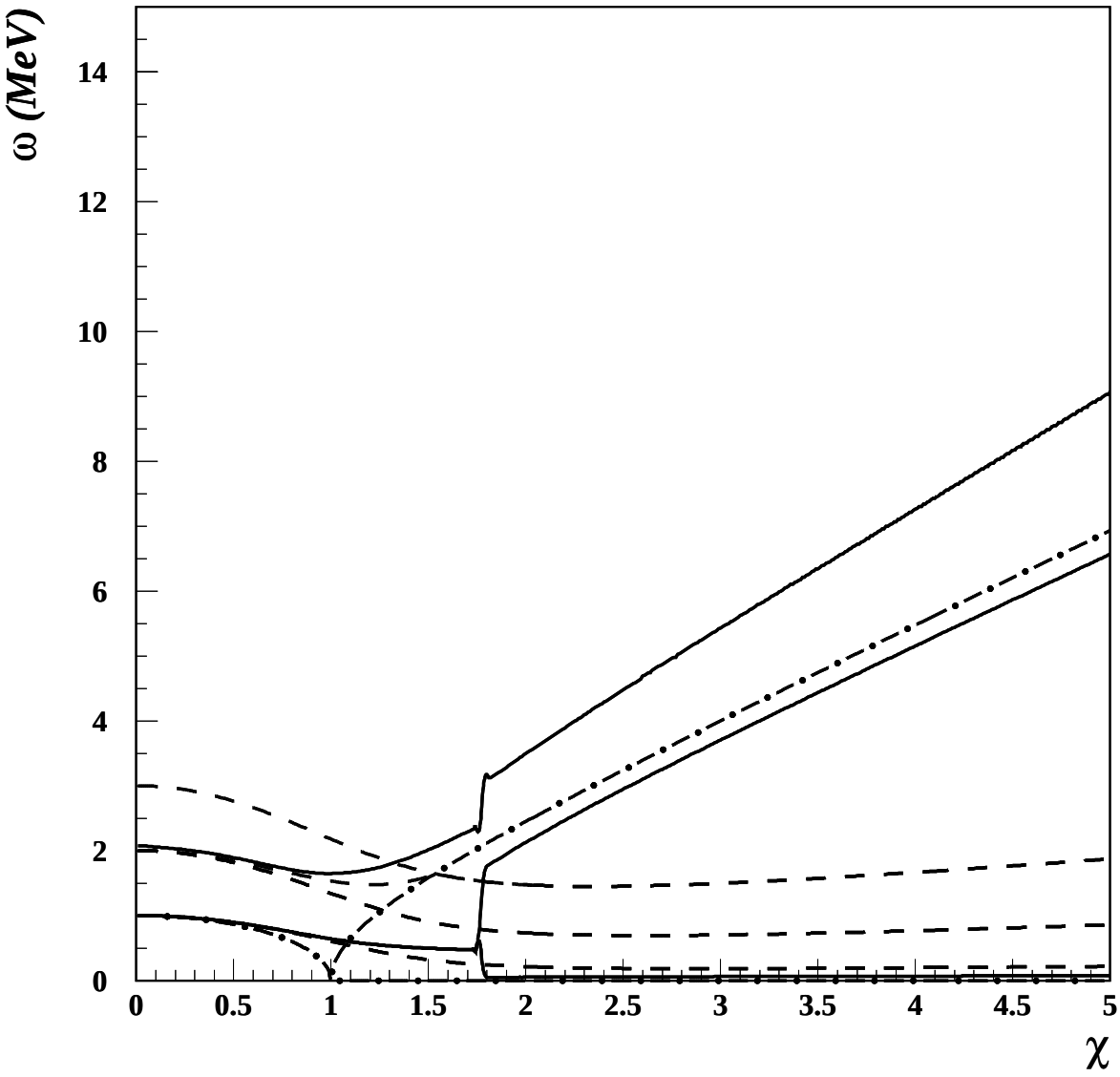

FIG. 5: The same as in Fig. 4, but for $N = 20$.

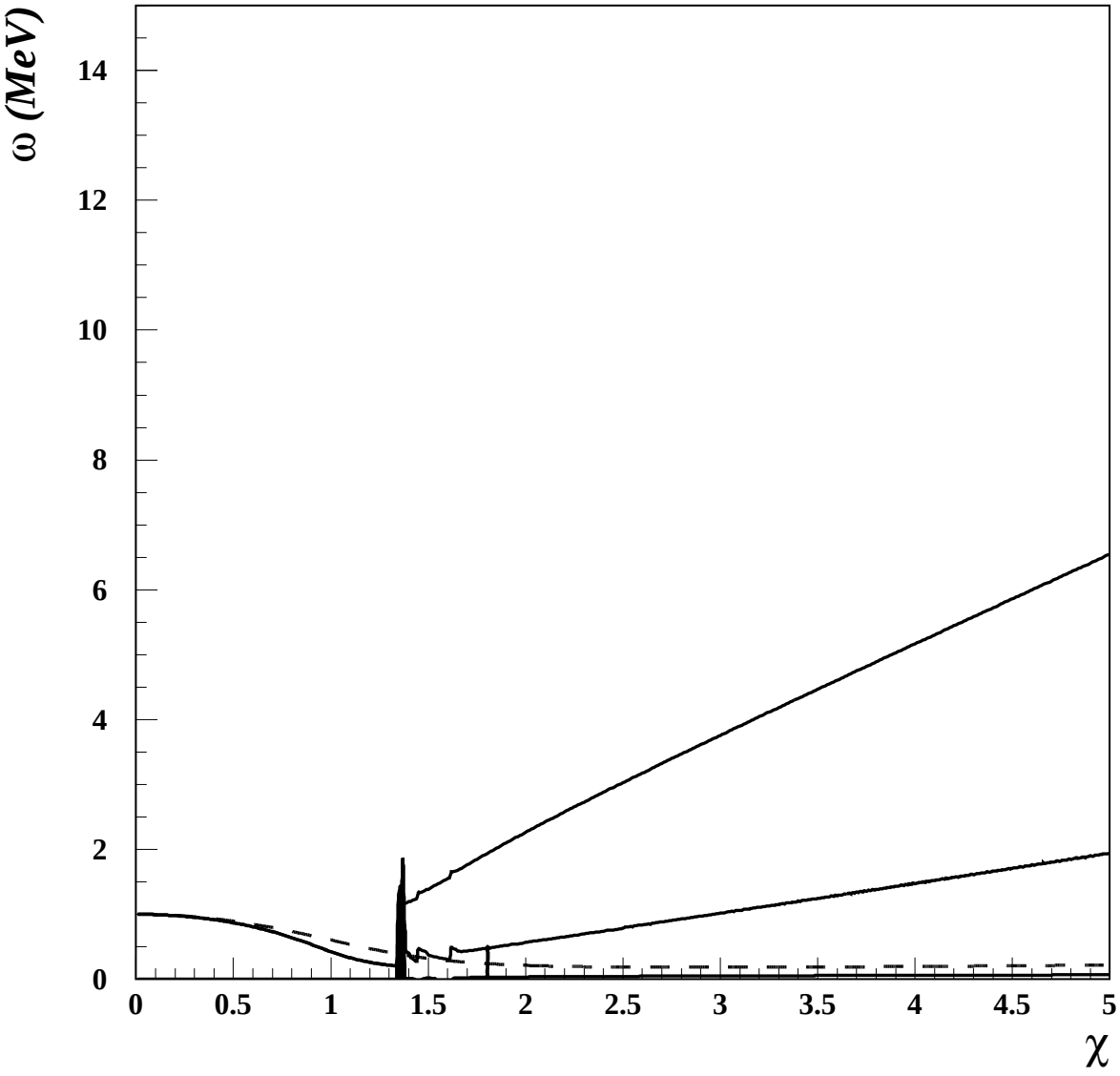

FIG. 6: r-RPA excitation energies versus the strength parameter χ, for $N = 20$, $\Delta\epsilon = 0.001\ MeV$ (solid lines). By dashes are given the lowest exact energies. The Goldstone mode appears at zero energy beyond $\chi \approx 1.4$. For $\chi \leq 1.4$ appears an unphysical mode of the order $\Delta\epsilon$ which cannot be distinguished from the abscissa on the scale of the figure.

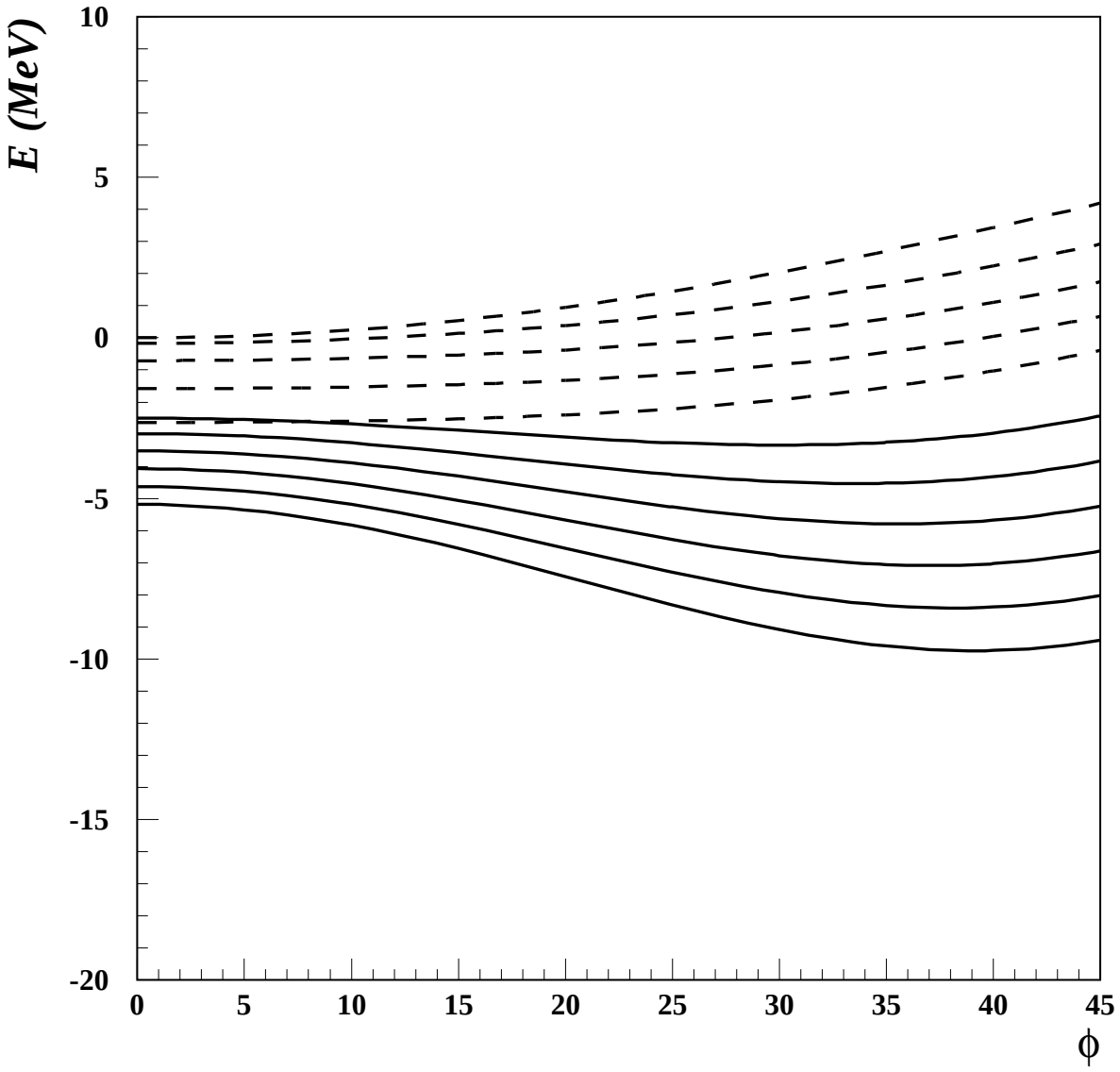

FIG. 7: The SCRPA expectation value of the Hamiltonian versus the angle ϕ, for $N = 10$ and different values of the strength parameter χ (from the top of the figure, $\chi = 0, 0.5, ..., 5$). By dashes are given the values for the spherical region and by solid lines for the deformed region.

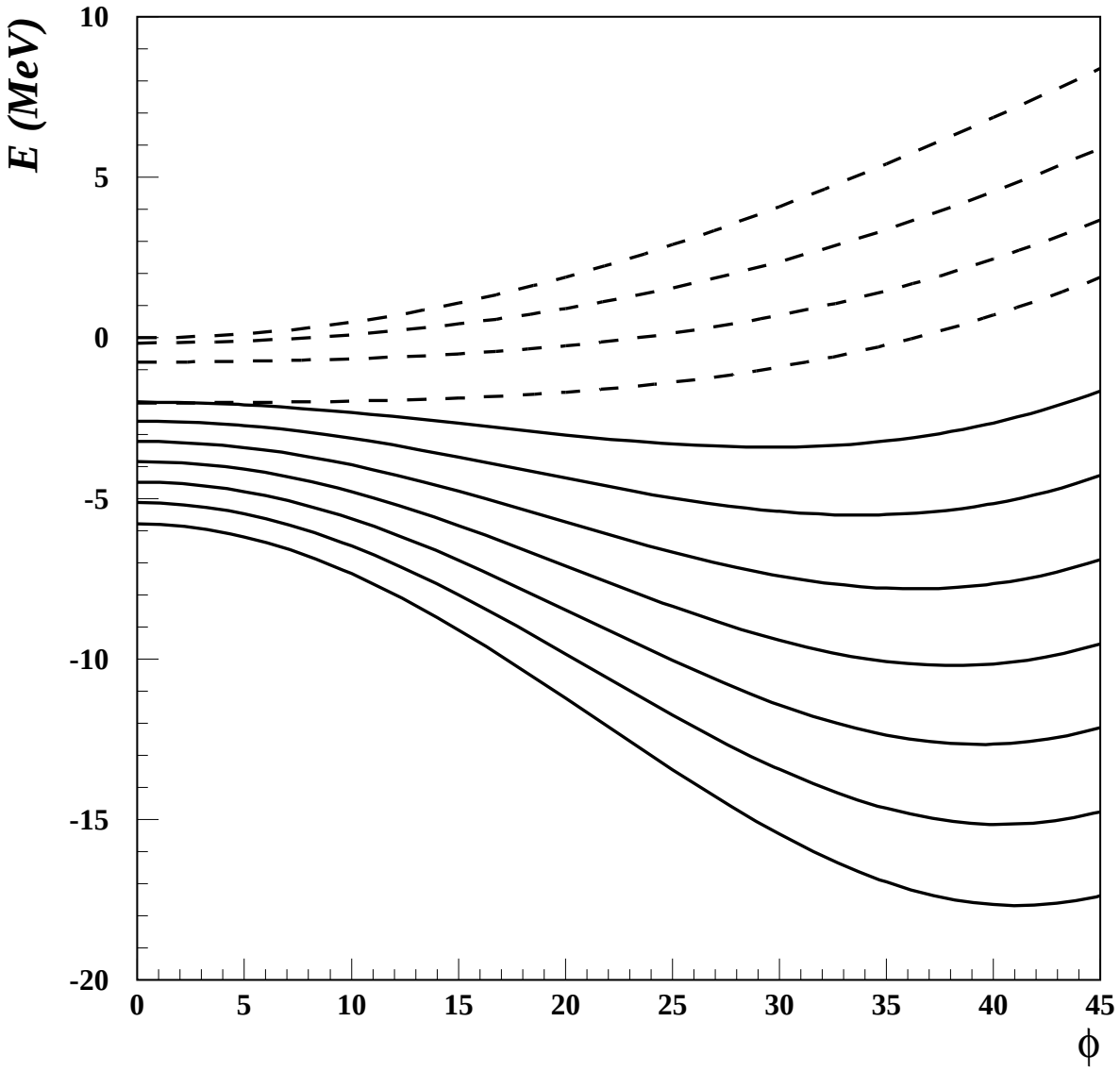

FIG. 8: The same as in Fig. 7, but for $N = 20$.

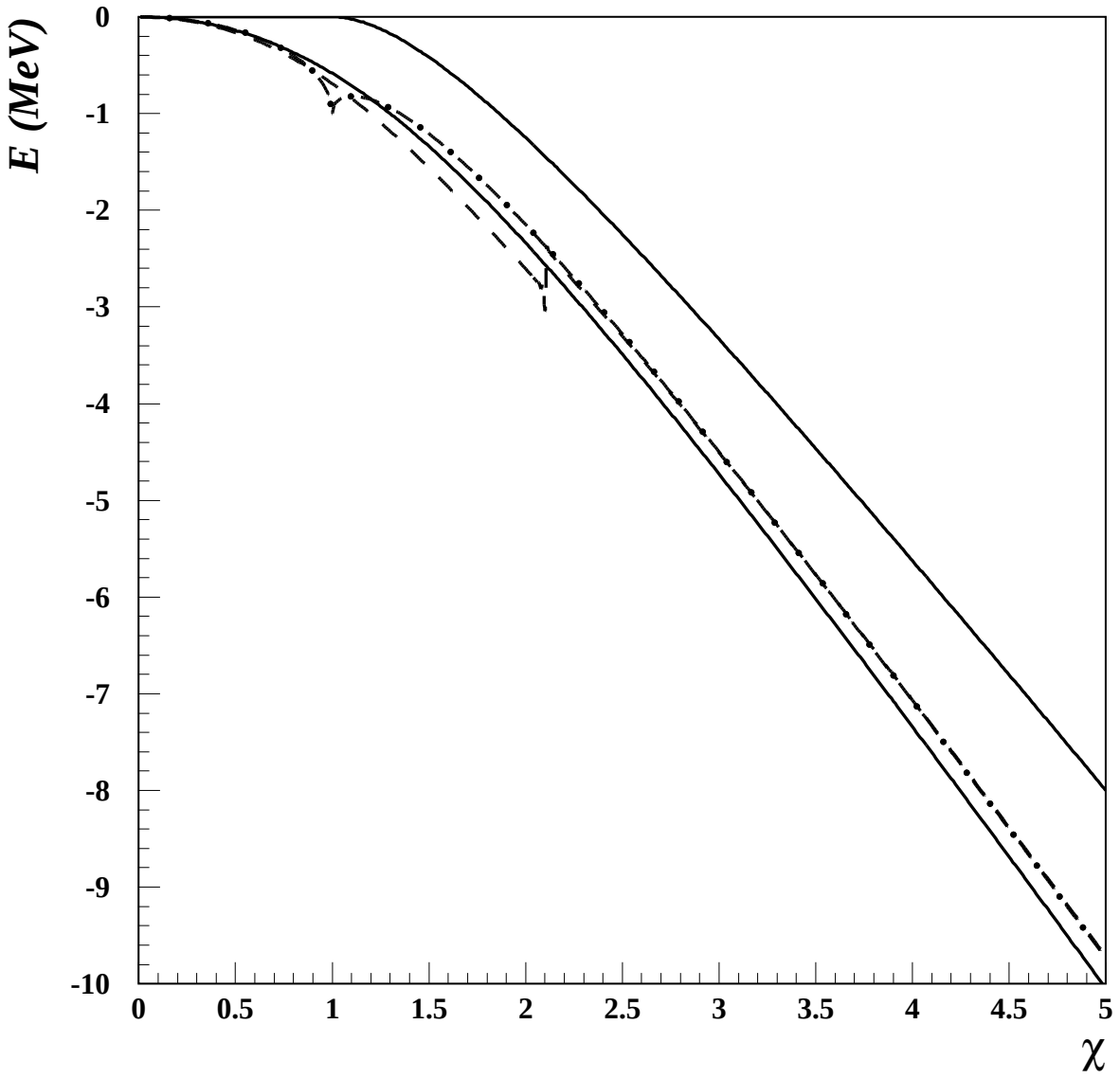

FIG. 9: The expectation value of the Hamiltonian versus χ for $N = 10$. By the lower solid line are given exact values, by dashes the SCRPA energies, by dot-dashes standard RPA results and by the higher solid line HF values. Once the SCRPA jumps to the deformed solution at $\chi \approx 2.1$ SCRPA and standard RPA are almost indistinguishible on the scale of the graph.

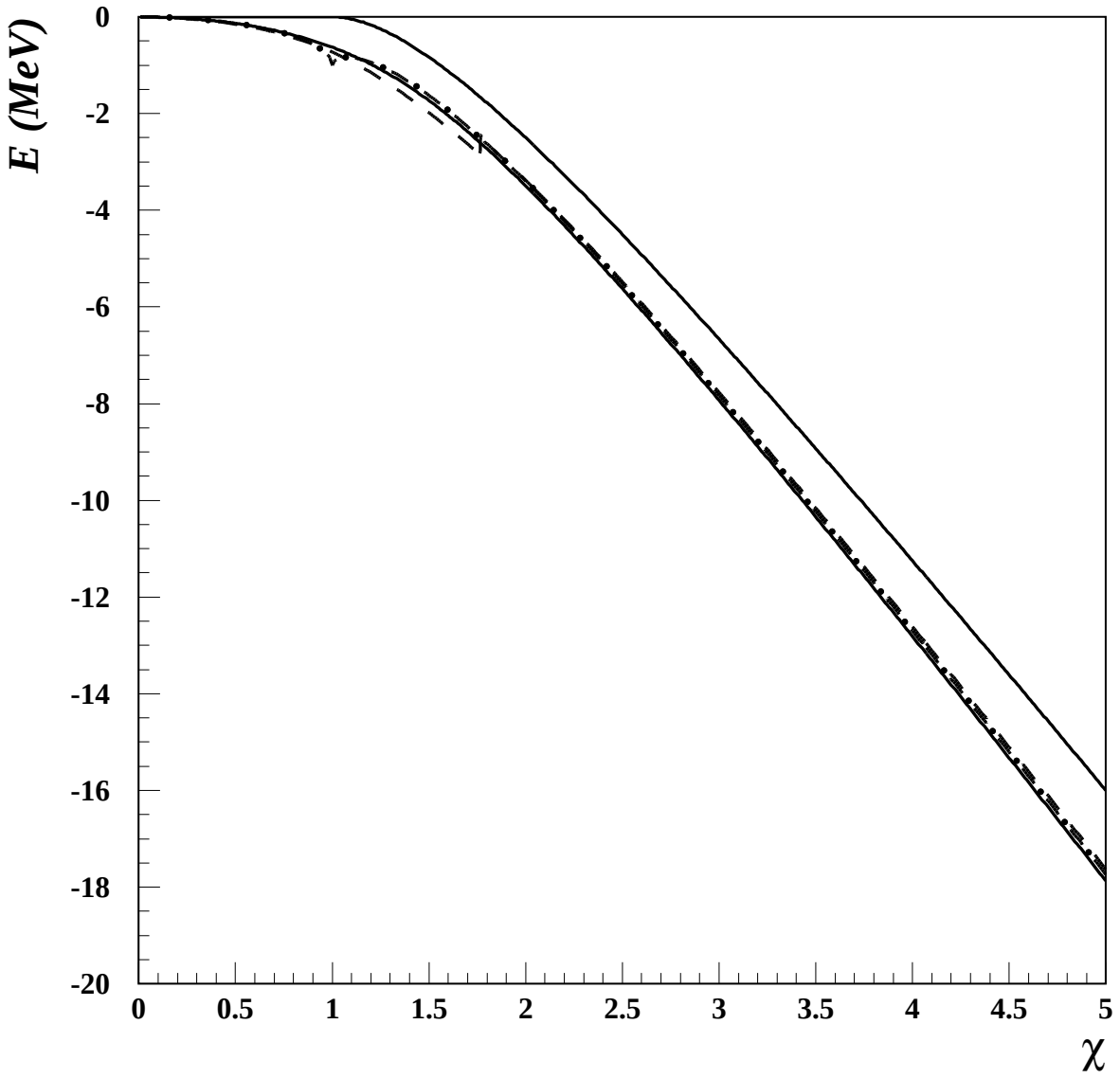

FIG. 10: The same as in Fig. 9, but for $N = 20$.

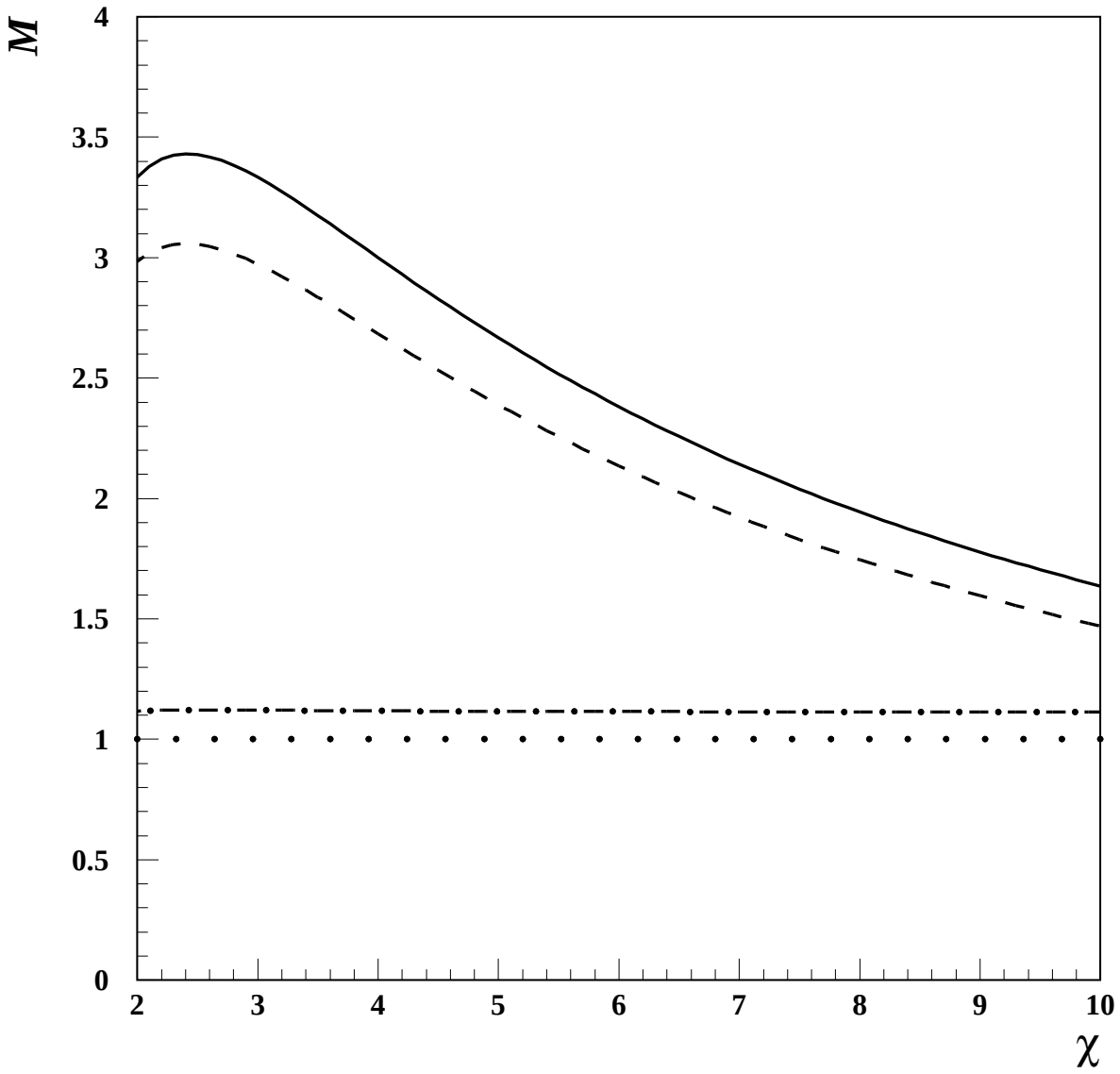

FIG. 11: The standard RPA inertial parameter versus χ (solid line), the inertial parameter from the exact energy spectrum (dashed line) and their ratio (dot-dashed line) for $N = 20$.

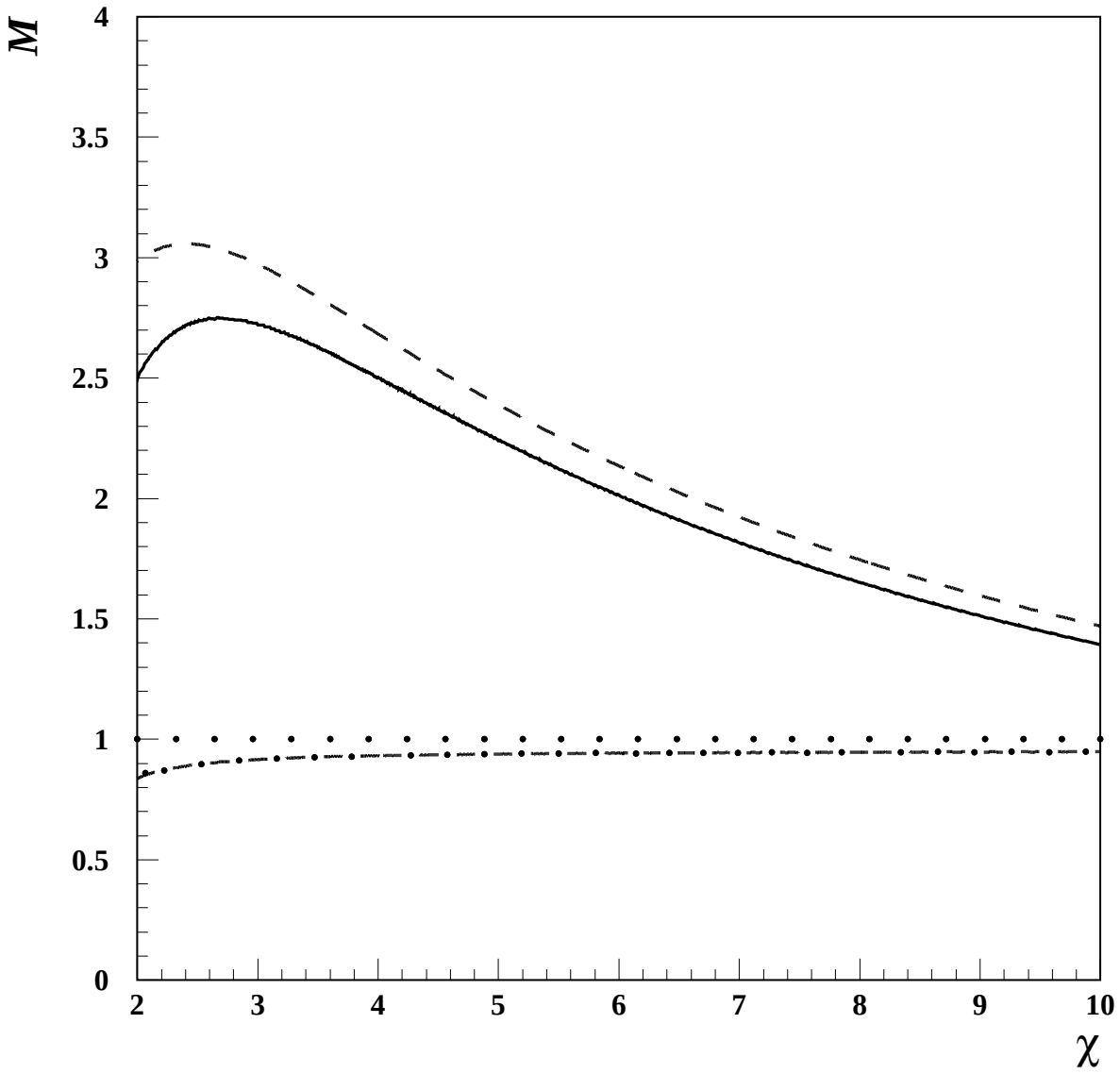

FIG. 12: The SCRPA inertial parameter versus χ (solid line), the inertial parameter from the exact energy spectrum (dashed line) and their ratio (dot-dashed line) for $N = 20$.

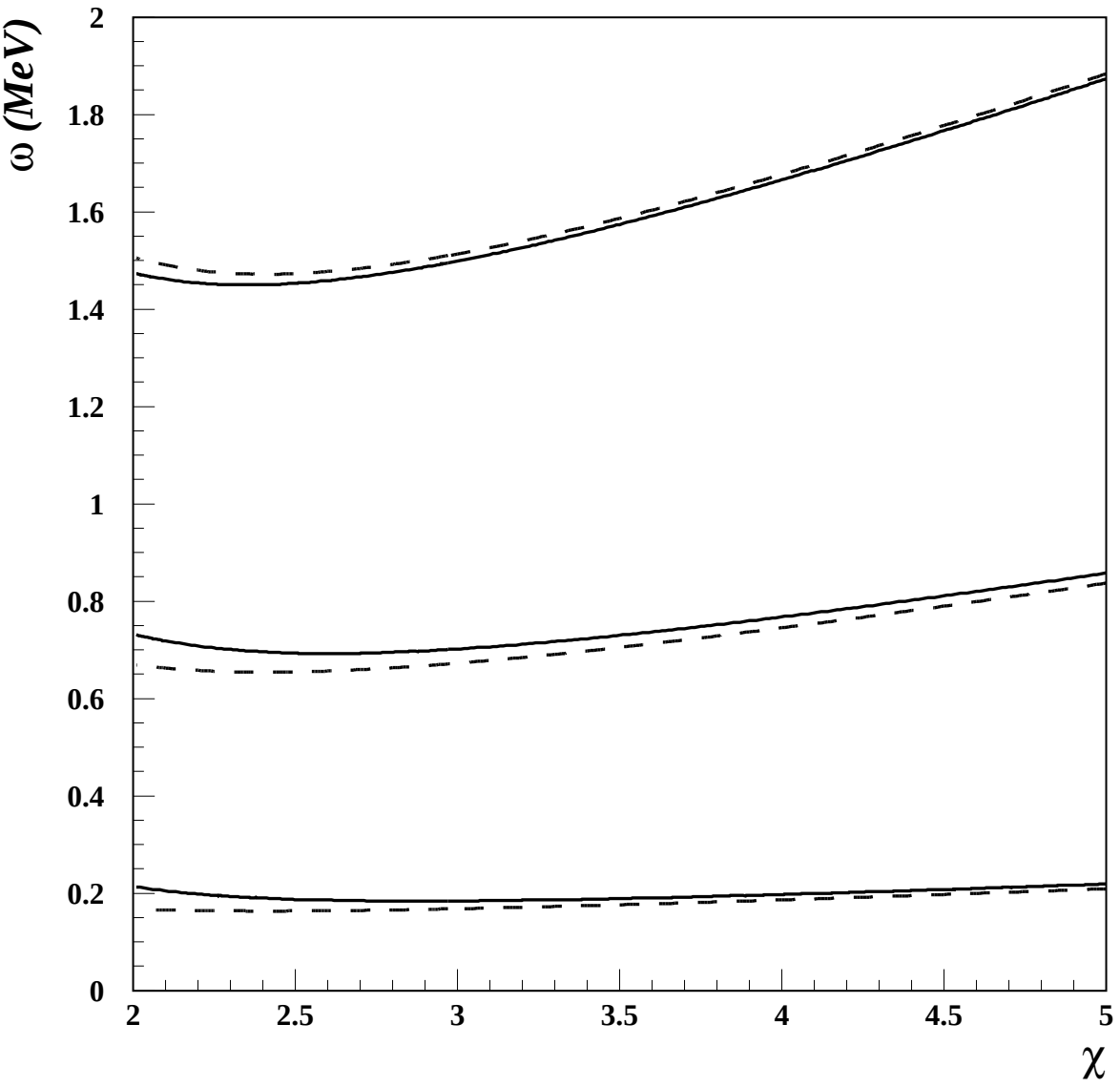

FIG. 13: The SCRPA rotational spectrum (dashed lines) and the exact energies (solid lines) for $N = 20$. The three levels correspond to $J = 1, 2, 3$.

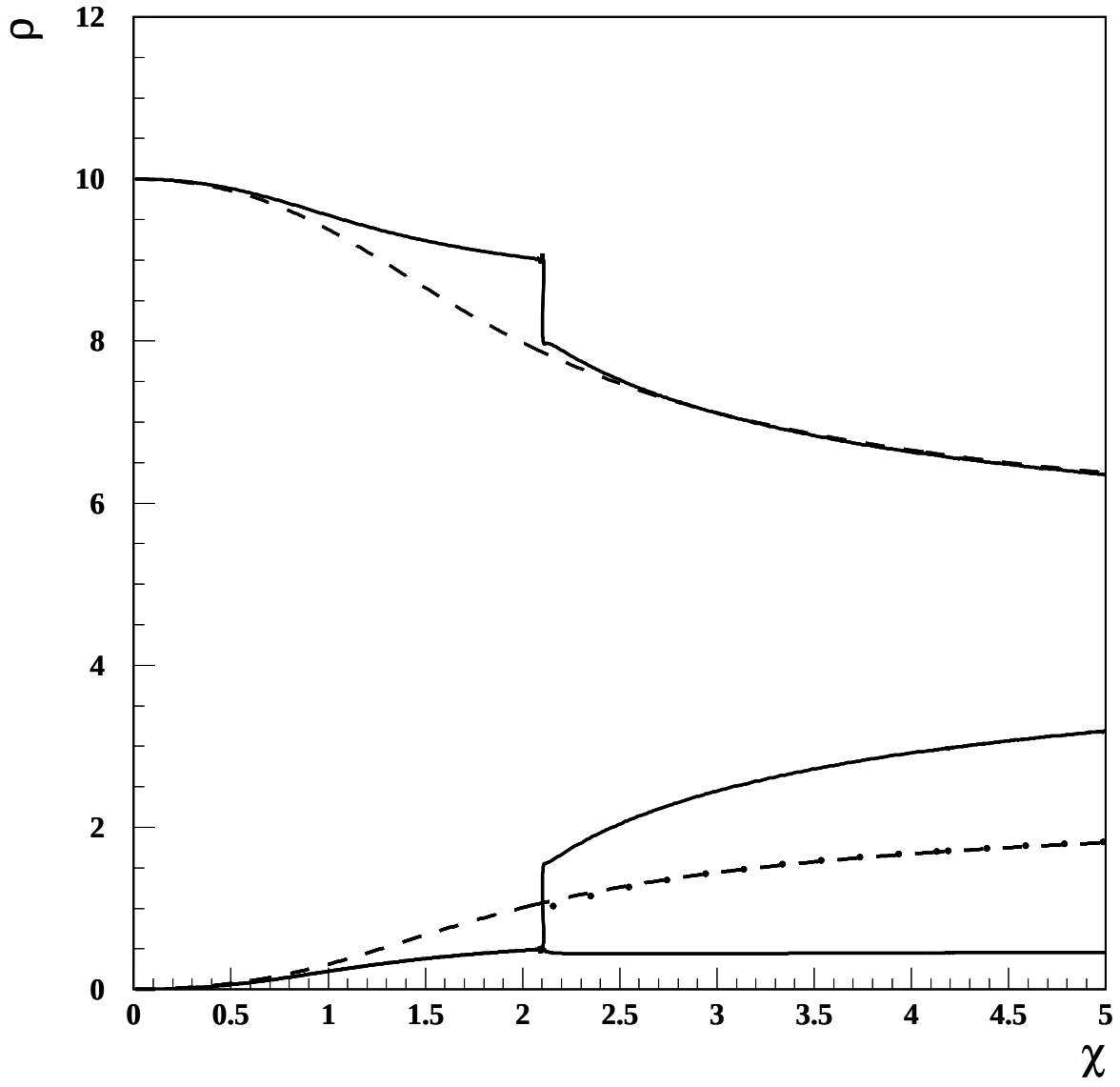

FIG. 14: The one body densities versus χ for $N = 10$. By solid lines are given SCRPA values and by dashes the exact results. The dotted line represents the average of two occupation numbers of states 1 and 2 for $\chi > \chi_{crt} \approx 2.1$.

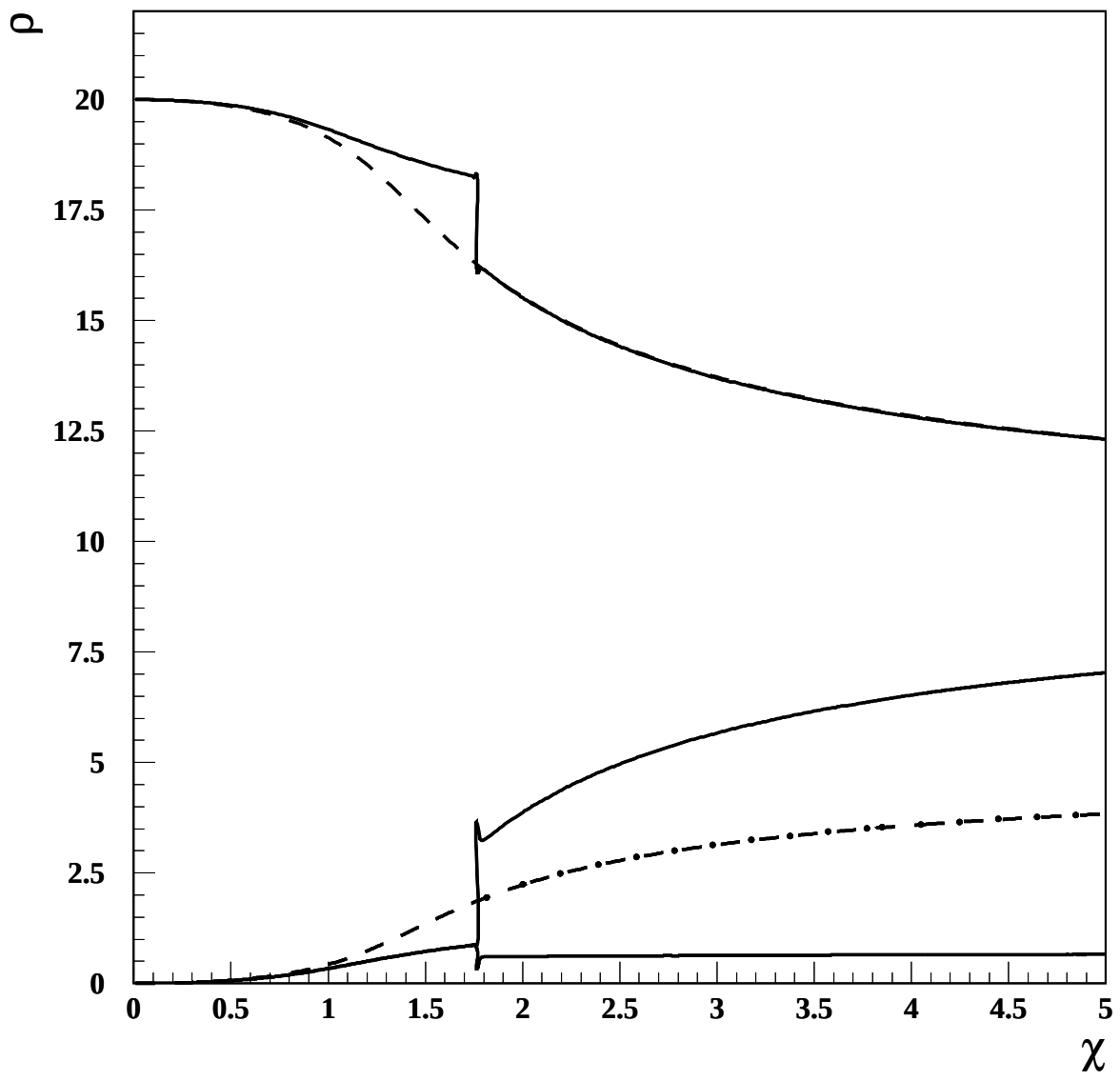

FIG. 15: The same as in Fig. 14, but for $N = 20$.